GEOLOŠKI ZAVOD SLOVENIJE
Dimičeva ulica 14, 1001 Ljubljana

Geotechnical, Geological, and Seismological (GG&S) Evaluations for the New Nuclear Power Plant at the Krško Site (NPP Krško II)

Paleoseismological trenches on the Libna Hill

Revision 1

LJUBLJANA, April 2011

Project:	Geotechnical, Geological, and Seismological (GG&S) Evaluations for the New Nuclear Power Plant at the Krško Site (NPP Krško II)
Phase:	1st, Addendum 1
Contract:	Consortium agreement 1130-167/07, Addendum 1
Investor:	Gen-Energija, d.o.o.
Consortium partners:	BRGM, GeoZS, IRSN, ZAG
Responsible for Consortium leader BRGM. Project leader:	Behrooz Bazargan Sabet
Responsible for task leader GeoZS. Director:	Marko Komac

Report/task

Responsible:	GeoZS	Miloš Bavec
Reviewer:	BRGM	Monique Terrier
Approbation:	IRSN	Stéphane Baize
Arch. No. GeoZS:		J-II-30d/b6b-4/3-d
Place and date:		Ljubljana, April 20th, 2012

	Baize Stéphane	IRSN
	Bavec Miloš	GeoZS
	Jomard Hervé	IRSN
Contributors:	Milanič Blaž	GeoZS
	Mišič Miha	GeoZS
	Poljak Marijan	GeoZS
	Rižnar Igor	Consultant
	Skaberne Dragomir	GeoZS

KEY WORDS: NPP Krško II, paleoseismology, trench, Libna fault, Libna Hill

List of Contents

List of Appendices

Appendix 1	External expert report	Daniela Pantosti
Appendix 2	Archeology report	S. Porenta & M. Novšak; Arhej d.o.o.
Appendix 3	Archeology supplement report	T. Verbič & S. Porenta; Arhej d.o.o.
Appendix 4	Displacement modeling	Branko Mušič; Gearh d.o.o.
Appendix 5	Mineralogy, Geochemisty in Granulometry data	D. Skaberne & M. Mišič, GeoZS
Appendix 6	14C dating report	R.E. Hatfield & D. Hood; Beta Analytic
Appendix 7	Luminescence dating report	F. Preusser; Stockholm University
Appendix 8	Comments on ESR dating results	P. Voinchet; Muséum national d'Histoire naturelle, Paris

1 SUMMARY

Three paleoseismological trenches were excavated within the zone of the Libna fault in fall 2010. The zone of Libna fault was interpreted to be between 150 and 200 m wide.

Selection of the sites on the Libna Hill was made upon significant geophysical campaign and a series of test pits.

Two of the three trenches were logged and interpreted in detail. One trench (trench #1) collapsed during the excavation. After the collapse the geometry of the other two trench walls was changed by building horizontal steps into the walls to avoid collapsing.

Trench #2 showed the most significant results, while trench #3 provided certain important additional information. Bulk of most important information is therefore summarized in the chapter *"Deformation pattern in Trench 2 and tectonic interpretation"*

General stratigraphy of the trenched area is (from oldest to youngest): Badenian (Lithotamnian) limestone, "residual clay" on the Badenian limestone, Plioquaternary gravel and sand, Plioquaternary silt, colluvium (at places) and modern soil.

In trench #2 it is interpreted that a dextral strike slip fault with certain vertical component is present. The general strike of the fault is NW-SE and the dip of striae indicates that the slip varies from 0° to 30° SE.

In trench #2, two main fault zones are observed along with an anastomosing system of accompanying fractures that cover the whole logged length of the trench (app. 26 m) and most probably extends also outside the trench toward ENE.

The Plioquaternary series is displaced in trench #2 and the displacement is significant.

Continuation of deformation upward into younger sediments in trench #2 (dated by archeological findings) is less obvious and several interpretations are presented in the report. In trench #3 the deformation does not propagate into the Plioquaternary succession but stops underneath.

The evaluation of displacement was only possible by combining results of additional geophysical survey (GPR and ERT) and observations in trench, and this was only possible along one of the two fault zones in trench #2. This displacement is evaluated to several meters (less than 10 m). Full displacement along the Libna fault is larger and distributed among other fault planes.

According to the current tectonic model, the potential displacement is not distributed evenly along the whole length of the Libna fault. It is concentrated mostly to differential folding along the Libna anticline and most deformation should be taken up there (on the Libna anticline).

ESR and OSL dates were obtained for the terrestrial Plioquaternary series during the course of this project that are surprisingly low (210.000 to 130.000 B.P.) for Globoko formation compared to the estimate of 1 - 2 million years before this project. At this stage, we cannot apply these age dates into the regional geological model (also outside Krško basin) so we decided to wait with further application until they are proven by independent analyses.

2 INTRODUCTION

Through Phase I of the project Geotechnical, Geological, and Seismological (GG&S) Evaluations for the New Nuclear Power Plant at the Krško Site (NPP Krško II), a series of evidences was obtained indicating that the Libna fault, a NW–SE trending strike–slip fault near the proposed sites for the NPP may be a capable fault (Fig. 1). The surveying described in this report followed a series of focused paleoseismological actions taken between 2008 and 2010 (described in the Phase 1 Geology report; Bavec, ed., 2010). The paleoseismological survey on the Libna hill is a contractual task controlled by the Addendum 1 to the main contact between GEN energija d.o.o. and the Consortium (BRGM, GeoZS, IRSN, ZAG).

Fig. 1 : Location of trenches on the Libna Hill with respect to the Libna fault (two lines indicate the approximated width of the fault zone) and the two proposed sites. The trench at Stari Grad (reported in 2008) is also shown.

In 2008, the first paleoseismological trench was excavated in the Sava alluvial plain across the western boundary of the geophysical anomaly band that is interpreted to be the Libna fault imprint. This trench crossed a segment of NW-SE strike-slip fault cutting the Pontian silts, but the expression of the fault in recent deposits was questionable. In detail, it has only been possible to observe an ambiguous step in the interface between Pontian silts and Holocene Sava alluvium, at the location of the fault zone in Pontian units. A set of linear "negative" imprints with individual lengths of 10-15 cm were also observed along this step, and it was suggested that these could have been generated by pebbles scratching the slickenside during a faulting event. A possibility of faulting activity during recent time has then been pointed out. However, no recent deformation was univocally interpreted and no deformation was observed propagating within the fluvial sediments (only 400 years old there). Because of this ambiguity of interpretation, together with the very young age of the upper fluvial sediments, it was then decided to perform additional investigations where the fault was suspected to cut older sediments in the Libna Hill.

Revision 1 of the report as presented here is taking into account 1) findings of the revision provided by GEN Energija (Technical report Designation TP-012, Revision 1 Comments on GG&S

"Paleoseismological trenches on the Libna Hill" Report), dated 19.12.2011, 2) independent review of Paul C. Rizzo Associates (Final Report; Independent technical review of the paleoseismological trenches on the Libna hill report), dated January 31th 2012 and 3) findings of the review meeting in Orleans, F. on December 13-14th, 2011 as documented in Minutes of meeting: Status and proposed activities on Libna geological feature.

3 TRENCHES ON LIBNA

Technical information and the team

After significant geophysical campaigns on the Libna hill and logging of several test pits, three trench sites were finally selected (Fig. 2): two trenches were excavated on the western edge of the Libna fault zone (trenches #1 and #2) where the geophysical signal of deformation was shown as most prominent, and one inside the Libna fault zone (trench #3). Trench #1 was dug first, but unfortunately collapsed a few hours after because of slope instability angle and poor soil conditions. To enable further work and primarily for safety reasons, the geometry of other two trenches was adopted by introducing a step in their vertical walls. Trench #3 was then successfully excavated in the Badenian limestone and its residual clay, with two non-deformed superficial layers of colluvium and Plioquaternary silt with pebbles, overlying it. Tectonic deformation observed in trench 3 was minor compared to the trench #2.

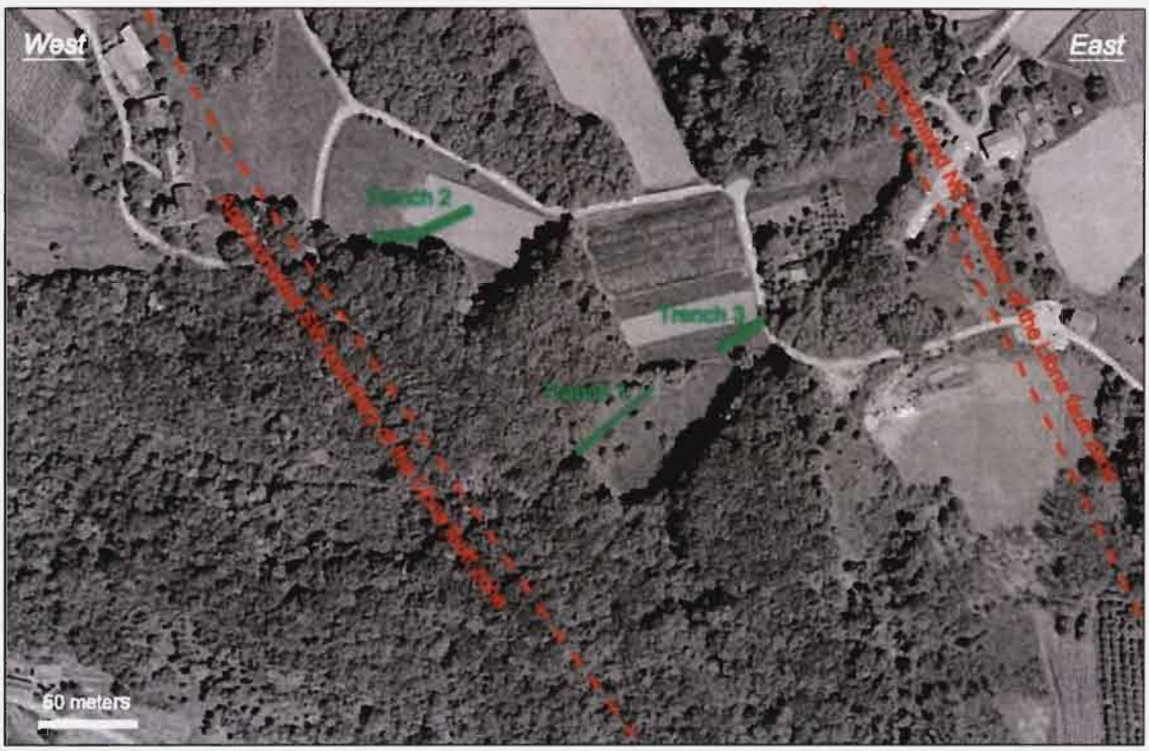

Fig. 2. Location of trenches on the Libna hill with respect to approximated outer boundaries of the widest Libna fault zone.

Trench #2 gave the most significant results with respect to the initial objective, which was primarily to validate or not the post-Plioquaternary activity of the Libna fault. Post-Plioquaternary activity of the Libna fault was proven.

	Corner coordinates				Lenght (m)	Orientation (azimuth°)	Depth (m)	Elevation [lowest - highest (m)]	
	1	2	3	4					
Trench 1	15°31'01.62"	15°31'01.68"	15°30'59.84"	15°30'59.90	13+37*	60	3,5 - 4,0	278	284
	45°57'05.93"	45°57'05.88"	45°57'04.89"	45°57'04.84"					
Trench 2	15°30'57.37"	15°30'57.46"	15°30'55.11"	15°30'55.12"	37,3	65 76 85	1,6 - 4,0	309	315
	45°57'08.93"	45°57'08.80"	45°57'08.46"	45°57'08.33"					
Trench 3	15°31'04.18"	15°31'04.28"	15°31'03.22"	15°31'03.25"	24	56	1,6 - 3,8	289	294
	45°57'07.05"	45°57'06.94"	45°57'06.61"	45°57'00.04"					

* excavated before collapse+planned

Table 1. Technical details of the trenches

Trenches were logged and interpreted by GeoZS (Dragomir Skaberne, Igor Rižnar, Blaž Milanič, Miloš Bavec) and IRSN (Stéphane Baize, Hervé Jomard) and with assistance of students of geology at the University of Ljubljana (Klemen Černič, Rok Brajkovič, Dejan Emeršič, Domen Bajec, Anže Merkelj). Responsible for this task is M. Bavec, GeoZS who also edited the report. The report is written by the whole professional part of the team.

Excavation started on 29th Sept. 2010 with trench #1, which collapsed the same day. Excavation for trench 3 was done on 7th and 8th Oct; gridding, logging and sampling lasted until 14th Oct, .2010. Trench2 was excavated between 11th and 13th of Oct. 2010. Gridding, logging and sampling was done between 12th and 22nd Oct. 2010. The first findings have shown potential high importance of results thus Daniela Pantosti (INGV Rome) was invited in the power of invited External Expert. She joined the team for the last two days in field and has reported her conclusions based on her field observations (Appendix 1). After initial interpretations were made, the team revisited the site for additional logging and sampling on 24th and 25th Nov. 2010.

Exact position of trenches is presented in Table 1 and in Fig. 3.

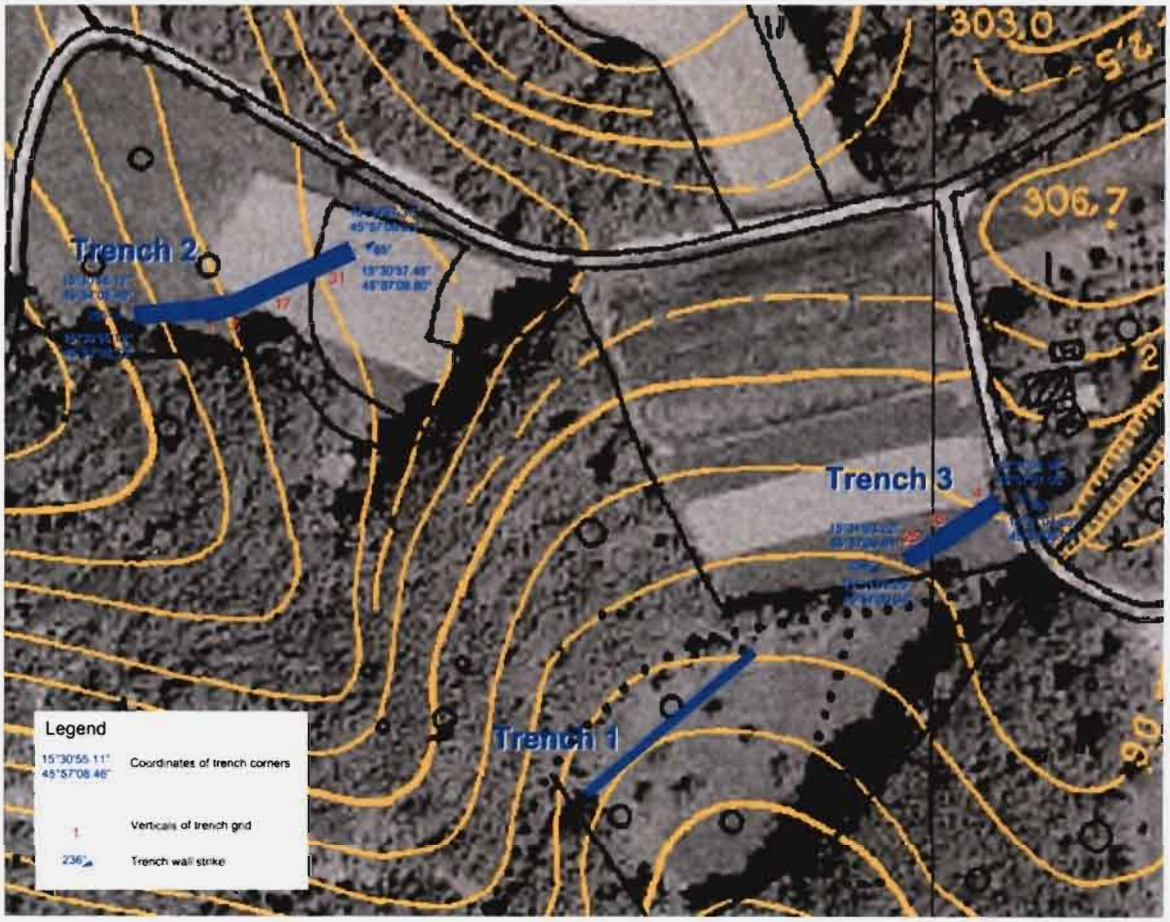

Fig. 3. Exact location of trenches on the Libna hill and geometric details.

During the course of excavation of the trench #2, archeological remains were discovered. The National Agency for Cultural Heritage (Zavod za varovanje kulturne dediščine Slovenije) was informed and protective archeological excavations were ordered. Archeological excavations were conducted by Arhej d.o.o and were lead by Matjaž Novšak and Andrej Porenta. The same company was consulted also regarding the finding of the silex artefact in the trench and regarding the archeological interpretation of the interface between the "cultural" and "geologic" layers. Archeological report is appended (Appendices 2 and 3).

Additional geophysical survey was ordered after first observations were gathered, to help evaluating displacement along the fault. It was conducted by Gearh d.o.o. and lead by Branko Mušič (Appendix 4).

This report presents the joined interpretation of the working group.

At the end of this report (section 5) the Consortium proposes further actions for clarification of activity and geometry of the Libna fault.

3.1 TRENCH 1

Trench 1 was planned to be excavated along the trace of the most prominent geophysicaly observed deformation (as well as trench 2) across a relatively steep slope. Unfortunately, by excavation the slope instability was initiated and the trench collapsed and was not logged (Fig. 4)

Fig. 4. Initiation of excavation in trench #1 (left) and the collapse of the wall that stopped the works (right). Note the contact of Pl,Q sediments with Badenian limestone on the right picture

3.2 TRENCH 2

3.2.1 General overview of findings in trench 2

Trench 2 can be described as the juxtaposition of 3 blocks separated by 2 main fault zones (Fig. 4). In the western side of the Trench, the fault zone 1 (FZ1) separates the Badenian limestone and its "residual clay" from the major mass of brown Plioquaternary silts (Fig. 5; Fig. 6) laying above the Plioquaternary (Pl,Q) gravel and sand. To the east, the brown silts are in tectonic contact with the gravel and sand (fault zone 2, FZ2). The section is topped by a modern soil layer (including the archeological layer) which seems undeformed by the post-Plioquaternary faults.

Fig.4. Trench 2 during cleaning and extraction of meteoric water. Fault zones FZ1 and FZ2 are marked.

One can observe a large amount of deformation features in the trench walls and floors, with fractures, fissures (filled with silt) and faults with apparent displacements. Vertical and horizontal sections present in the fault zone 1 (FZ1) area show that deformation is distributed along many fractures that juxtapose many blocks of silts, clays and PlQ gravels. This great number of tectonic lenses suggests that the cumulative displacement is substantial (more than just a few meters). The second fault zone separates the silts, from the weathered gravel and sand, and coincides with the thickening of the modern soil, and the location of an iron-age house discovered during the trench analysis. Faults and fractures are generally subvertical, or steeply dipping to the ENE. Together with the main faults, the secondary network of fractures forms an anastomosing system. In addition, the stratigraphic conditions in the trench do not allow direct estimation of the offset along the faults (FZ1 and FZ2). Namely, the base of the (Pl,Q) silt in the structural block between the fault zones (FZ1 and FZ2) is not known and the silt there is much thicker than in the easternmost block, where the base of

the silt is observed. All these observations, together with the finding of a gently dipping striation on the fault planes indicate that deformation is associated with dextral strike-slip movements (with a non-negligible vertical component) along the general strike of the Libna fault (NW – SE).

A general observation is that faults and fractures cross all the series (Limestone, PlQ gravels and silts) up to the soil interface which seems to be undeformed.

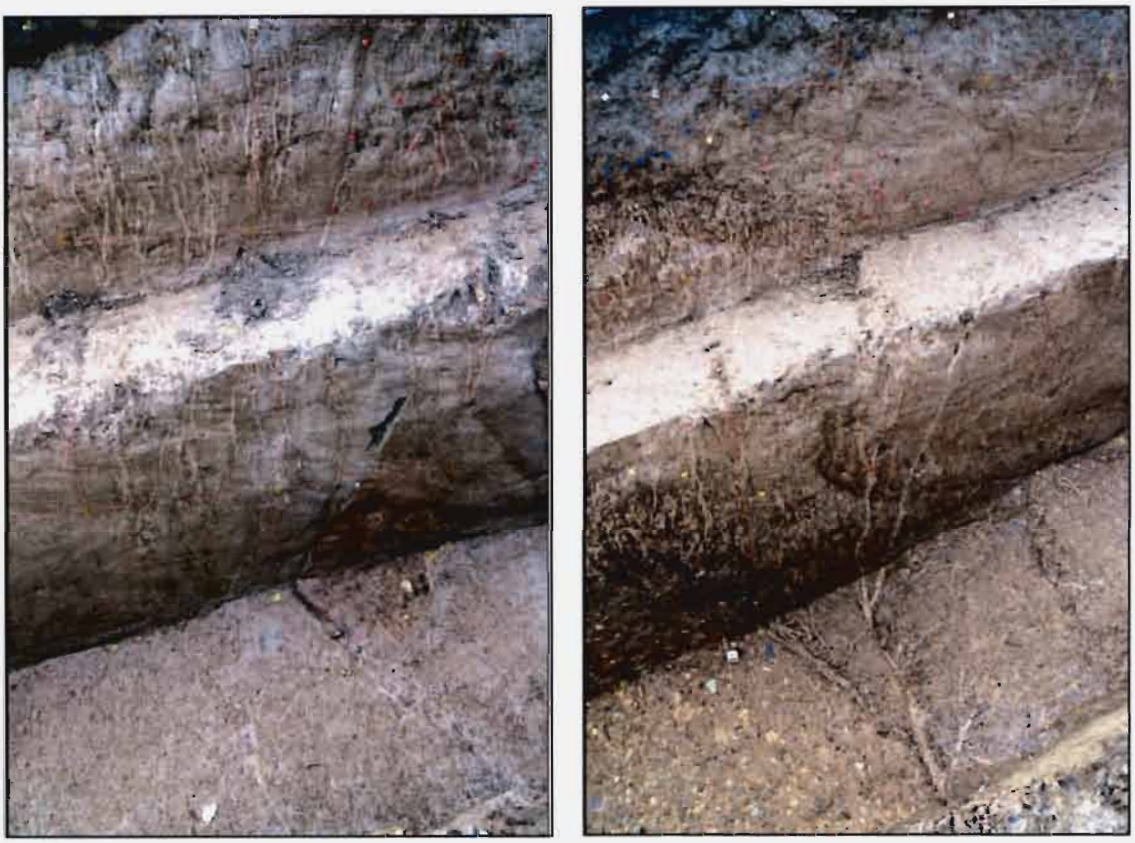

Fig. 5 : The two fault zones exposed in the Trench #2; fractures and fault planes are underlined by red flags. To the left, FZ1 between the limestone with the "residual clay" (right) and the brown silts (left) is made of various lenses (the most prominent is the red one, at the bottom of the trench, which involves the pebbles of the Plioquaternary gravel and sand). To the right, FZ2 between Plioquaternary gravel and sand (left) and brown silts (right) is also made of various strands with large variation in strike.

It is important to underline that the most significant fault plane within FZ2 ends beneath the iron-age soil with soil infiltrations downward into the fault gouge. The infiltration can be interpreted as an infill of an open crack, which could have been formed during a deformation event. In strike-slip "environment", the identification of deformation events (like earthquakes) is not an easy task. Classical criteria such as "fracture upward terminations" beneath successive laminations, "unconformities" or even "colluvial wedges" (see Mac Calpin, 2009 for a synthesis) were not observed here. Some authors (e.g. Lienkaemper and Williams, 2007) also define fissure fills as features unique to coseismic displacements. However, if the observed infiltration features were indeed opening of fault plane and fissures with soil infiltration (V-shaped cracks) it would suggest that coseismic deformation could have occurred on these faults during or just after the soil

formation. The presence of such open cracks near the soil base, not erased by the pre-archeological erosion period (ie. during glacial period) would also indicate that the observed deformations are quite young (post glacial period). At least two "non-seismic" interpretations of V-shaped cracks genesis are also possible of which the following cannot be rejected by our findings: 1) opening of cracks due to mass movement (the modern surface is inclined at about 10°) and 2) desiccation. A plausible interpretation of soil infiltration is also infiltration of fault gouge by bioturbation for which no open cracks are needed or simply alteration of fault gauge by water infiltration. For discussion on these interpretations see section 3.2.4. of this report.

Our primary position based on the data presented in this report is that the significant deformation ends in the stratigraphic unit called here the Plioquaternary silt and that the deformation does not propagate into historic layers above. The age of the last deformation is thus controlled by the age of the PlQ silt (younger than PlQ silt and older than the Hallstatt culture). A further alternative, which is not definitely demonstrated, favors a tectonic (also coseismic) interpretation of the modern soil infiltration into the fault gouges, which dates the latest deformation to Holocene. This interpretation is presented by the consulted external expert Daniela Pantosti (Appendix 1).

Another impacting difference in potential interpretation is related to the genesis of the whole (or a part of the) silt unit (called here the Plioquaternary silt) as colluvial and to the position of the silex artefact within this silt. According to interpretation of D. Pantosti (Annex 1), the silt may be colluvial thus the silex artefact (200.000 to 2.500 BC) may have been deposited within the colluvium (synchronous with deposition) and thus predates the deformation along the fault. This interpretation is not well demonstrated as to begin with, the silt is definitely of fluvial origin (except possibly the upper 10-20 cm). There are other possible interpretations of the artifact position such as infiltration into a crack that has not been opened coseismically, or the one suggested by the archeological expert that the artefact could have been pushed downward into the silt by bioturbation (see Appendix 2) or by other means (for discussion on artifact position see section 3.2.4).

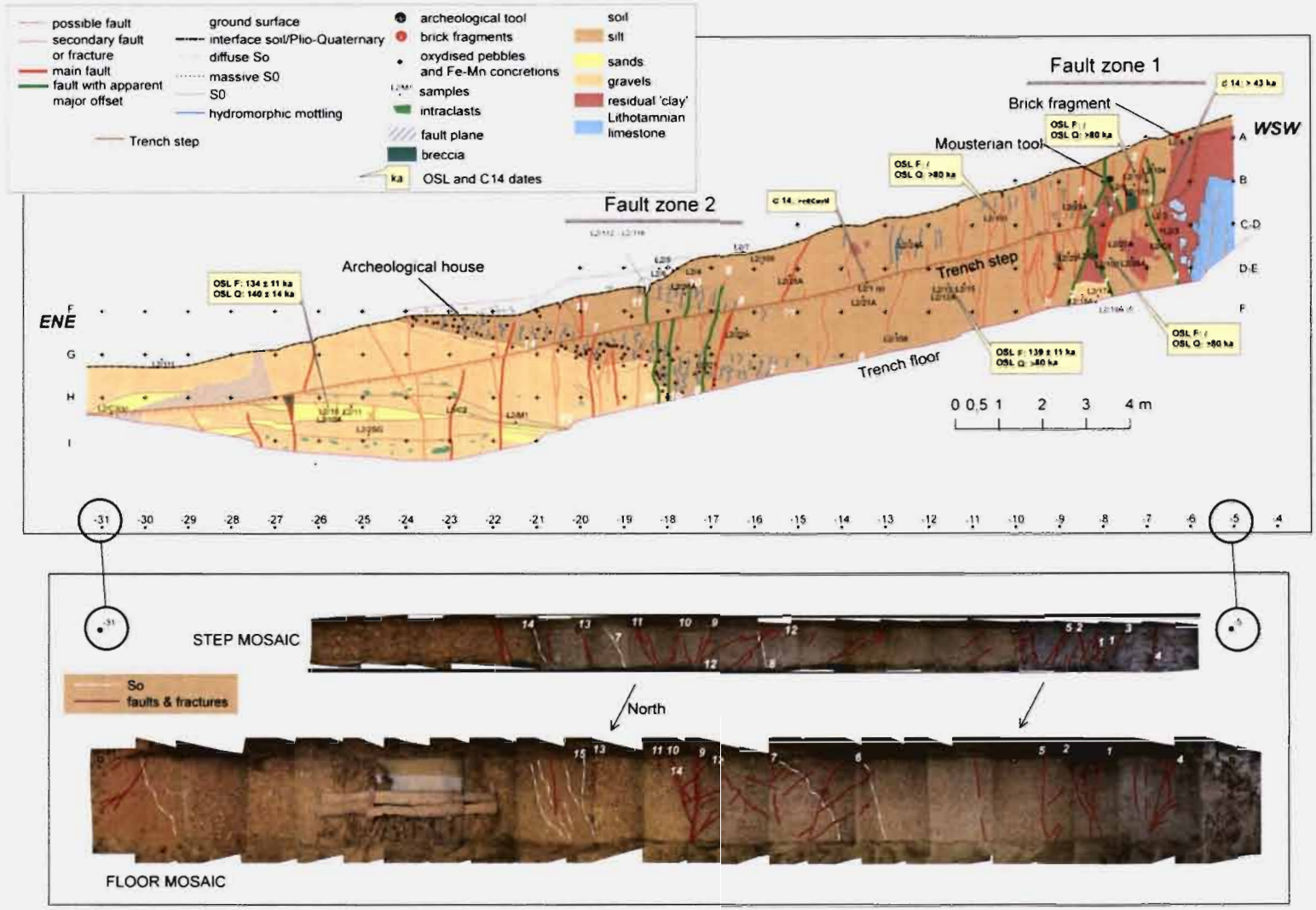

Fig. 6 The log of Trench 2.

The absolute age dates for the PlQ series (the Globoko aloformation) were obtained after several past attempts for the first time within this project (and for the first time in the region) and are unexpected. ESR (from the Globoko locality but for the same geologic aloformation) and OSL dates (from the trench) coincide relatively well and estimate the age at around 210.000 and 130.000 years BP respectively. A leap from previous age estimates (ranging from 0.3 to 5 million years; e.g. Swan et al., 2004) and by most authors to between 1 and 2 million; e.g. Šikić et al., 1979; Verbič, 2004) is enormous and we cannot fit these new age estimates into the regional geological interpretations. For that, we are using the new age dates more as one of options and not as solid fact. The age – dating results are discussed in section 3.2.3 of this report.

The displacement along the fault was evaluated solely by a model, based on bedding plane orientation in trench and on the geophysical evaluation of continuation of the lithological units outside the trench. The piercing points for such an evaluation were not found within the trench at both sides of the fault, and further excavation was not possible due to archeological protection of the area. Cumulative displacement along one of the two fault zones (the one with enough "geophysical contrast"; FZ 2; maybe the one with less displacement accumulated) is estimated at the order of magnitude of several meters (less than 10 m).

The SW wall of the trench 2 was logged in detail, while opposite wall was used for gathering additional information. The floor and the "step" (created to enable stability of wall) of the trench were also logged (Fig. 6).

3.2.2 Detailed description and sedimentological interpretation of sedimentary units

Three main sedimentary sequences are outlined in trench2. The oldest and lowermost sequence consists of the Badenian limestone overlain by the "residual clay". The middle and most prominent sequence consist of gravel, sand and silt of the Plioquaternary age. The most recent sequence is a soil of the Holocene age. Badenian limestone, overlain by the "residual clay" is in the fault contact with the Plioquaternary silt but the Holocene soil forms a cap covering the "residual clay" and Plioquaternary gravel, sand and silt.

3.2.2.1 The Lithotamnian limestone - Badenian

Lithotamnian limestone of the Badenian age crops out at the WSW side of the trench 2 against FZ1 and continues to the west in the Libna hill. It is the oldest formation observed in the trenches. In the trench 2, it was exposed in the thickness of up to 2.5 m. This homogenous limestone is in tectonic contact with the brown silt of the Plioquaternary age at the 5.6 to 6.0 m (FZ1). It appears affected by shearing and it is intensely weathered and covered by a thick sedimentary cover of red silty clay (referred to as the "residual clay") in the westernmost part of the trench. The latter is eroded at the WSW side of the trench (outside the logged section), and the limestone is covered there only by modern soil (Fig. 7;).

Fig. 7 Badenian limestone is covered by the "residual clay", while at the WSW tip (trench back, behind the man) of the trench it is covered only by a recent soil.

Macroscopically, the limestone is described as white Lithotamnian bindstone and calcarenite with fragments of bivalves, bryozoans and foraminifers encrusted by red algae (*Lithotamnian)* that may form rhodolites. The limestone is also intensively karstified forming very uneven corroded surface with deep indentations also filled by the "residual clay" (Fig. 8).

Fig. 8 . The Lithothamnian limestone is massive, fractured, weathered and intensively karstified. The contact with the "residual clay" is very uneven and corroded. There are isolated corroded fragments of limestone in the "residual clay". The SW wall of the trench, between app. 1-8 m.

3.2.2.2 The "residual clay"

The massive silty clay referred here to as "residual clay" is lying above the karstified surface of the Lithotamnian limestone and is overlain by soil (Fig. 8). It is up to 1 m thick and is eroded in the WSW end of the trench (Fig. 7). The color of the "residual clay" is light brown to brown (5YR4-5/6). It

consists on average 81 % silt, 18 % clay and 1 % sand grain size fraction (Appendix 5). According to these data the clay should in fact be named silt but is kept here with quotation marks for easier division with other lithologic units in the trench. Its mineralogical composition is: quartz 10 %, plagioclase 2 %, muscovite/illite 55 %, chlorite 28 % and goethite 6 % (Appendix 5). Muscovite is weathered to less well crystallized illite.

Sedimentological interpretation: The "residual clay" is interpreted as paleosoil – chromic (brown) cambisol developed on the Lithotamnian limestone during its exposure and before deposition of the Plioquaternary sediments. The presence of allochtonous, most probably aeolian maternal, as known in many soils of "terra rosa" in the Mediterranean region is described in section 3.4.1.

3.2.2.3 The gravel and sand of the Globoko Formation – Plioquaternary

Gravels with lenses of sand occupy most of the trench 2 between 18 and 31 m. The gravels are overlain by brown silt. At 18 m, the gravels are in a tectonic contact with the brown silt (Fig. 6). Gravely and sandy lithofacies are forming about 3.7 m thick sequence in which five sedimentary units were identified (Fig. 9).

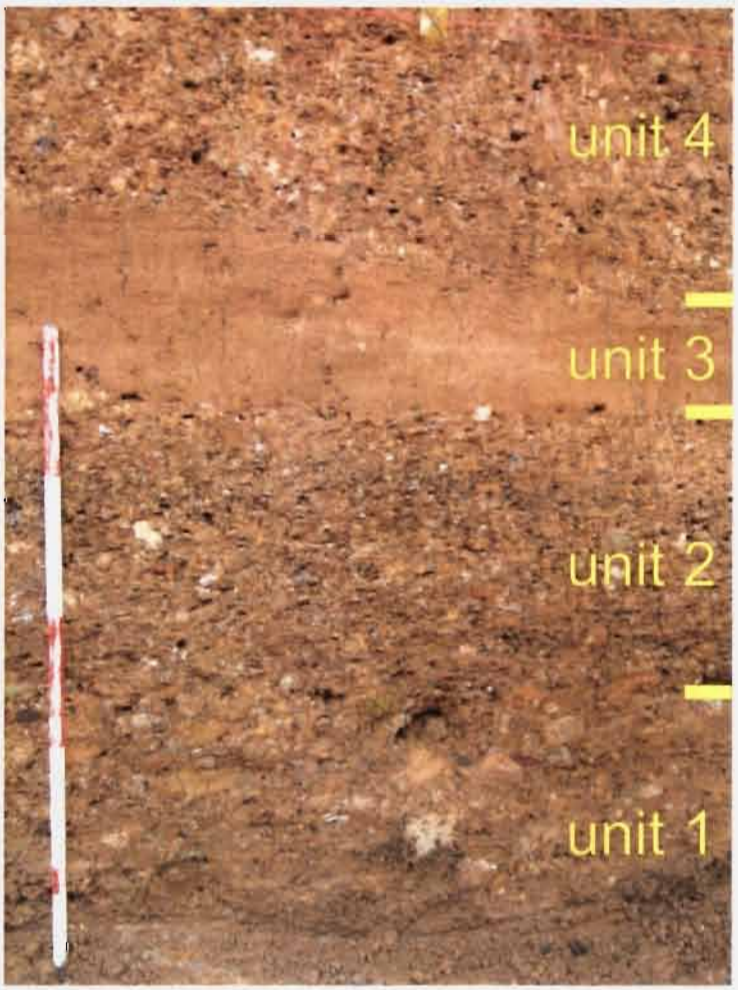

Fig. 9 The succession of units 1, 2, 3 and 4. A fracture filled by silt in the upper right side. The SW wall of the trench, around 25 m.

The colors of these gravely lithofacies are mostly pale to moderate yellowish orange (10YR5-6/6). Their texture is grain-supported containing 70 to 80 % of pebbles and 20-30 % of sandy-muddy

matrix. (Percents are given as an area, not weight estimation.) Pebbles are predominantly poorly sorted and well rounded. The composition of the pebbles is given qualitatively, not quantitatively. There are only pebbles of non carbonate composition. Lithic pebbles are prevailing over quartz ones. The lithic pebbles are: siliciclastics (red to violet sandstone and siltstone, brown sandstone, siltstone and rare quartz conglomerates), volcanic rocks and tuffs (mostly reddish and green) and cherts. The siliciclastic and tuff pebbles are mostly very weathered and can easily disintegrate. In some units larger (up to 40 cm) sandy and silty intraclasts are present (rip-up clasts).

Unit 1 was observed in the lowermost part of the trench between 21.2 m and 25.4 m in the thickness of up to 45 cm. It consists of massive, sandy gravel (SG/m) lithofacies with about 70 % pebbles and 30% sandy-muddy matrix. The pebble sizes are 30 (2-150) mm (mean(min-max)). There are some intraclasts of sand and silt up to 40 cm across. The sandy-muddy matrix consists of 48 % sand and 52 % mud. It contains 68 % quartz, 2 % plagioclase, 2 % microcline, 17 % muscovite/illite, 8 % chlorite and 2 % goethite.

Unit 2 - massive sandy gravel to gravel (SG-G/m) lithofacies with lenses of sand - overlies with sharp contact the unit 1 and was traced between 20.8 m and 31.0 m. It is up to 75 cm thick. The sandy gravel to gravel contains 70-80 % pebbles and 20-30 % sandy-muddy matrix. The pebble sizes are 15-20 (2-60) mm. The sandy-muddy matrix contains 52 % sand and 48 % mud that is composed of 61 % quartz, 2 % plagioclase, 2 % microcline, 20 % muscovite/illite, 13 % chlorite and 2 % goethite. The massive sandy gravel to gravel lithofacies is interbedded with lenses of medium sand that are up to app. 1.5 m long and up to 25 cm thick. They are concentrated between 26.6 m and 28.8 m, where they are dissected by faults. It contains about 1 % of quartz pebbles of sizes between 2 and 30 mm mostly concentrated in a thin bed.

Unit 3 overlays the unit 2 with a sharp contact. Its upper boundary with unit 4 is erosional (Fig. 9). The thickness of the Unit 3 varies from 0 to 40 cm and is thinning to the WSW. In the Trench 2 it was traced from 20.3 m to 31.5 m. Unit 3 consists of a massive medium sand (mS/m) lithofacies with app. 1 % of quartz pebbles of 2 to 20 mm in grain size. It consists of 66 % pebbles and sand, 28 % silt and 6 % clay (Appendix 5). The mean grain size is 0.27 mm. Sand is composed of 58 % quartz, 2 % plagioclase, 3 % microcline, 25 % muscovite/illite, 9 % chlorite and 2 % goethite (Appendix 5). The unit 3 is in a lateral contact with the unit 2 and is cut by a fault at 26.6 m. Between 23.0 m and 26.6 m the Unit 3 is nearly horizontal but between 20.3 and 23.0 m it is inclined for about 10° to the WSW and completely eroded between 21.8 and 22.4 m (Fig. 10).

Fig. 10. Unit 3 is nearly horizontal in the ENE part and becomes inclined for about 10° to the WSW direction. It is completely eroded in the WSW part of the Trench 2. The SW wall of the trench, between 21-24m.

Unit 4 has erosive lower and upper boundary. The unit can be followed from 20.3 m to 26.6 m and is up to 40 cm thick. It thins to the WSW, but to the ENE it is completely eroded. Unit 4 consists of

massive, sandy gravel to gravel (SG-G/m) lithofacies. It consists of 70-80 % pebbles and 20-30 % sandy-muddy matrix. The pebble sizes are 15-20 (2-70) mm.

Unit 5 has erosive lower contact and overlays unit 3 in the ENE part, and Unit 4 in the middle part of the Trench2, respectively. The contact of the Unit 5 with the overlying silt of the Globoko Formation is normal and distinct and can be traced from the ENE part of the trench until 18th m, where it ends up against the fault. Unit 5 is in lateral tectonic contact with the stratigraphically younger silt of the Globoko Formation there (Fig. 11). The Unit 5 is up to 180 cm thick and is formed by a massive, sandy gravel to gravel (SG-G/m). It consists of 70-80 % pebbles and 20-30 % sandy-muddy matrix. The pebble sizes are 30 (2-150) mm. It contains sandy and silty intraclasts up to 20 cm in size (Fig. 12). Larger clasts are oriented parallel (long axis) to the lower bedding plane in the lower part of the Unit (Fig. 13). The sandy-muddy matrix contains 55 % sand and 45 % mud composed of 59 % quartz, 3 % plagioclase, 2 % microcline, 22 % muscovite/illite, 11 % chlorite and 3 % goethite. The lower erosive contact with the Units 3 and 4 is nearly horizontal from 23.0 to the ENE end of the trench and inclined 15° to the WSW from 23.0 to 20.3 m. In the upper 10 to 20 cm of the Unit 5 there is about 30 % of black pebbles coated and impregnated by Fe-Mn oxide and hydroxides (Fig. 14).

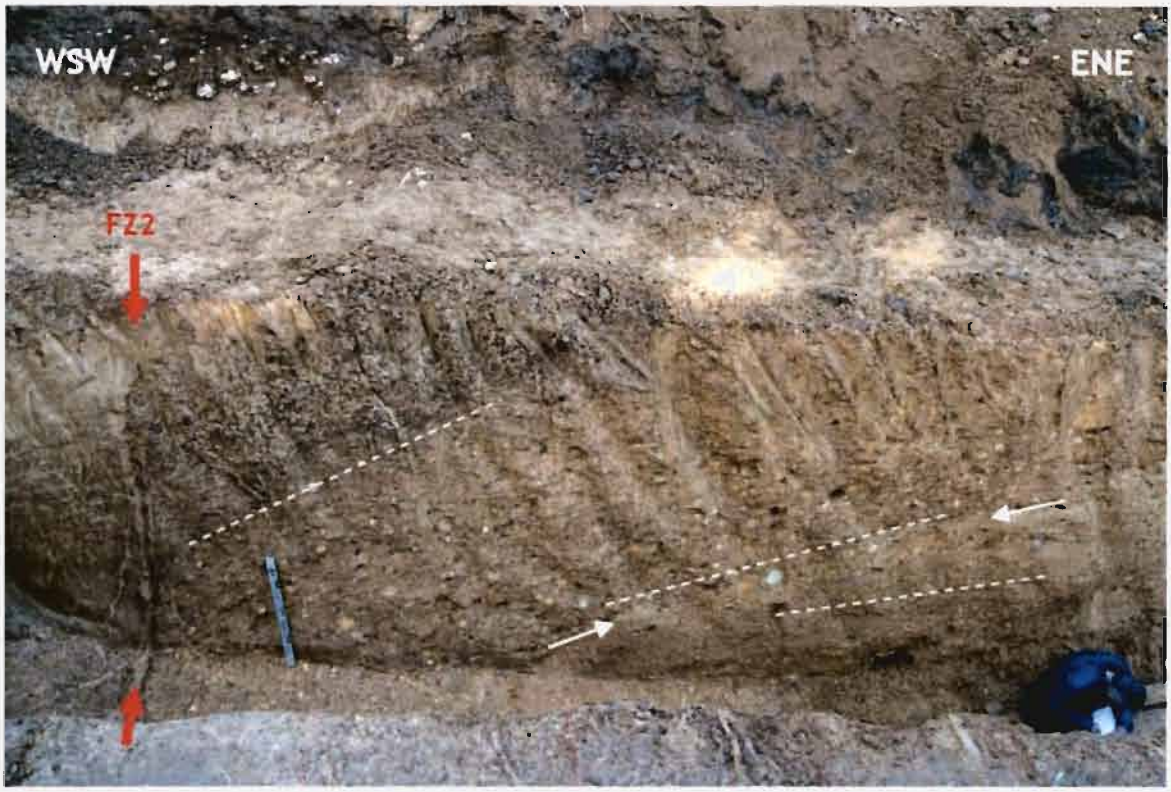

Fig. 11. The normal and distinct upper contact between the unit 5 and overlaying silt of the Globoko Formation and lateral a fault contact (FZ2) between them. The lower part of the unit 6 (just above the topmost dashed line) is the horizon rich in black Fe-Mn nodules and pebbles. Note the change of dip between the units. "Angular unconformities" of pure sedimentary origin – cross stratification are common in such sedimentary environment, while inclination (15° to the WSW) of obscured lamination in silt is of tectonic origin.

Fig. 12 The unit 5 contains among other pebbles also sandy and silty intraclasts in the lower part. The SW wall of the trench, around 23 m.

Fig. 13 Larger clasts are oriented with long axis parallel to the lower bedding plane in the lower part of the Unit 5. A fracture filled by silt. The NE wall of the Trench 2, around 22 m.

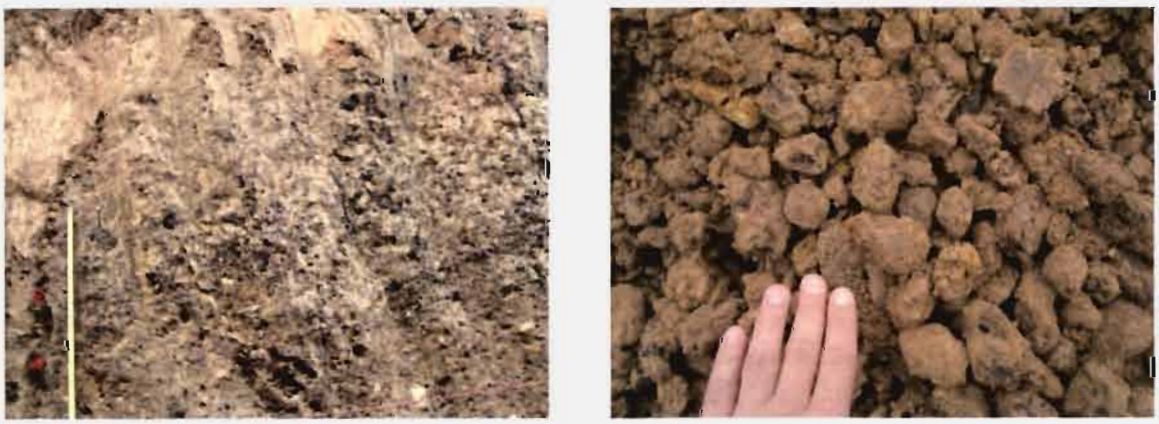

Fig. 14 The normal upper contact between the Unit 5 and the overlaying silt of the Globoko Formation (left). Black pebbles coated and impregnated by Fe-Mn oxide and hydroxides are present in the uppermost part of the unit 5 (right) while in the lower part of the silt a layer with black Fe-Mn nodules and pebbles is a dominant feature. The SW wall of the trench, around 18 m.

Sedimentological interpretation: Sedimentological interpretation of the Units 1 to 5 is presented along with interpretation of the silt of the Globoko formation at the end of the next subchapter.

3.2.2.4 Silt of the Globoko Formation – Plioquaternary

Silt of the Globoko Formation normally overlays the Unit 5 between 18.0 and 24.6 m. At 18.0 m it is in tectonic contact with the Unit 5 along the FZ2 (Fig. 11), and at about 6.0 m (Fig. 15) it is in tectonic contact with the Badenian Lithotamnian limestone along the FZ1.

Fig. 15: The upper part of the Plioquaternary silts in the FZ1 area (fault strands are underlined by red flags), including the position of the Mousterien tool (white flag).

The Silt is covered by modern soil. Thickness of the (PlQ) Silt Unit is about 8.0 m. It contains in average 83 % silt, 10 % clay and 7 % sand and pebbles ((Appendix 5) and consists of 43 % quartz, 5 % plagioclase, 5 % microcline, 33 % muscovite/illite, 12 % chlorite, and 2 % goethite (Appendix 5). Predominant color is moderate yellowish brown (10YR5/4). It is massive to obscurely laminated, and includes two horizons with numerous black Fe-Mn oxide nodules and mottles in the lower part (Fig 14). The obscured lamination and horizons with numerous black Fe-Mn oxide nodules and mottles shows 15° inclination to the WSW. The most prominent is 50 to 70 cm thick lower horizon overlying the Unit 5 (Fig. 14). It contains up to 30 % of black Fe-Mn oxide nodules and pebbles in the lower part but their quantity diminishes upward. Black Fe-Mn oxide nodules and pebbles are 15 (2-100) mm in size. Beside black pebbles it contains also quartz and lithic pebbles. About 90 cm up the sequence there is the second, less distinct horizon with the black Fe-Mn oxide nodules and mottles about 50 cm thick (Fig. 16). The silt is marmorized (Fig. 17) about 1.5 m in depth, most prominently along the older roots bioturbations that are nearly vertical and is bioturbated by modern roots, worms and moles under the modern soil (Fig. 18). In many cases the modern bioturbation follows the pre-existing one or runs along tectonic fractures (Fig. 18, 19). Near the contact with the Badenian

limestone (7.8-8.8 m) the tectonic inclusion of the red "residual clay" and the Plioquaternary gravel is found at the bottom of the trench (Fig. 5).

Fig. 16 The massive to obscurely laminated silt with the upper horizon containing black Fe-Mn nodules and mottles. Those are more frequent in the upper then in the lower part. The NE wall of the trench, between 13.5-15.5 m.

A silex artefact, possibly being used as (man-made) silex-tool was found included in the uppermost part of the Silt Unit, and the silty matrix drapes it (Fig.20). According to the archeological expertise (Appendix 2a), the artifact is poorly shaped, and cannot be dated precisely. Such artifacts can date anywhere within the Mousterien (Paleolithic; between 200.000 and 30.000 years b.c.) and can be followed up to the Eneolithic (2.500 years b.c.). Its position in the sedimentary succession is discussed in section 3.2.4.

Fig. 17. Tectonically fractured, bioturbated and marmorized silt under the modern soil. The SW wall of the trench, between 8.5-10.5 m.

Fig. 18. The modern roots bioturbation. In the upper left side it follows a fill of tectonic fracture. The SW wall of the trench at about 7 m.

Fig. 19. In places modern bioturbation follows the older one or a tectonic fracture.

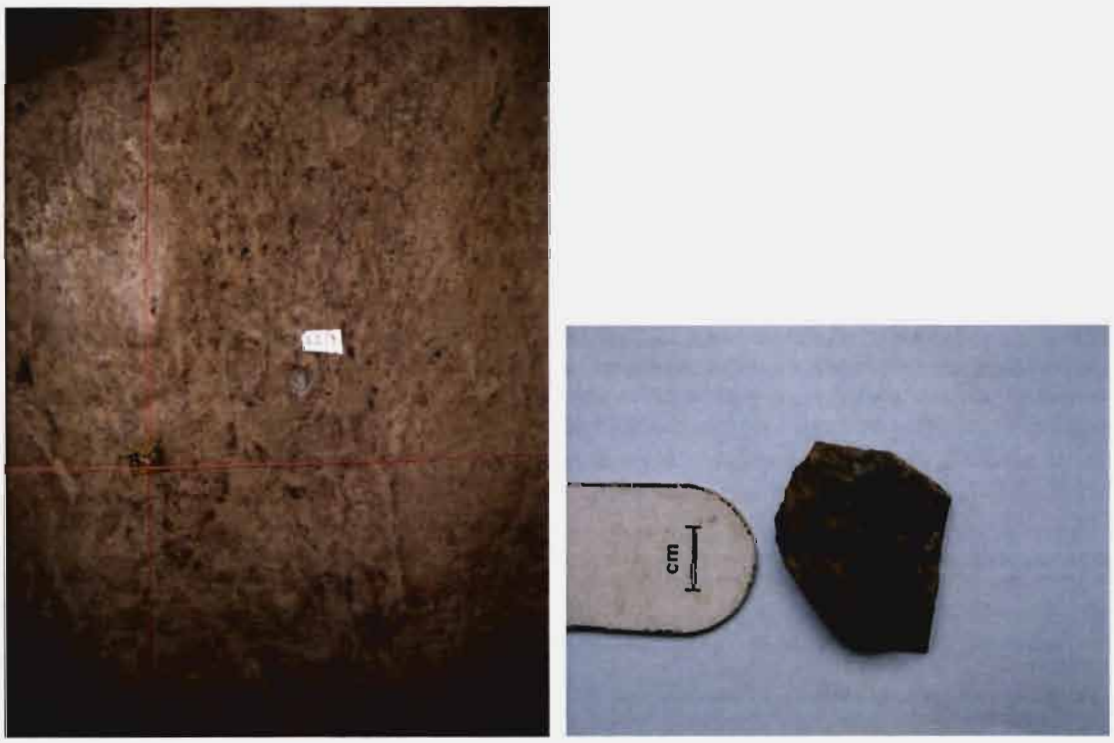

Fig. 20. The artifact found 80 cm below the overlaying Holocene soil within the Plioquaternary silt. Left: position with regard to the trench grid. Right: the artifact.

Sedimentological interpretation of the Plioquaternary succession (altogether): sediments of the Globoko Formation outcropping in the Trench 2 are divided into two lithologic and genetic units.

The gravel and sand of the Globoko Formation (described here as units 1 to 5) are interpreted as fluvial deposits of high energy, predominantly coarse-grained bed load braided stream. The units 1, 2 and 3 are most probably a part of a composed longitudinal to traverse bar formed by falling flow regime connected to a dropping of water level in a stream. The Units 4 and 5 are interpreted as gravel bars and bed forms cannot be interpreted in more details.

According to the facies, the massive Silt unit with poorly expressed lamination is clearly continental and a general opinion is shared inside the team, stating that it has been deposited by fluvial processes and corresponds to overbank sediments. The reason is that macroscopically similar facies are present as (thinner though) interbeds in the Plioquaternary fluvial gravels at the Globoko reference outcrop.

Sedimentological data (field observations and granulometry + chemistry + mineralogy) converge toward interpreting the fluvial origin of the silt although rejection of colluvial origin is not possible without any ambiguity.

One of allogenic processes of extrabasinal origin such as tectonic, eustacy or climate change (or possibly also an intrabasinal autogenic sedimentary processes) probably caused an avulsion of the stream from the place under consideration. The area became an alluvial flood plain on which the Silt Unit of the Globoko formation was formed. In the meantime, during a depositional hiatus, the pedogenic processes under an influence of a high ground-water level left their imprint in the uppermost part of the Unit 5 in a form of black pebbles – pebbles coated and/or impregnated by Fe-Mn oxide and hydroxides. After some time, floods of a distal stream began to deposit silt that now forms the Silt Unit of the Globoko Formation. The rate of silt sedimentation was low so that it allowed continuation of the same type of pedogenic processes forming the lowermost silty part of the Globoko Formation, the horizons with black Fe-Mn nodules, pebbles and mottles, interpreted as pseudogley horizons. The rest of the flood plain silty deposits were also strongly influenced by pedogenic processes, but only the ones in the lower part of the silt succession seen in the Trench 2 lasted long enough to produce the second (upper) distinct pedogenic pseudogley horizons.

The interpretation of the silt being fluvial overbank sediment is supported by field sedimentological observations, and converge with the synthesis of mineralogical, geochemical and granulometric analyses (Appendix 5). The uppermost 10 to 30 cm of the succession lack conclusive evidence of fluvial sedimentation thus there is a possibility that in this part the silt has been reworked on slope and deposited as colluvium.

3.2.2.5 Holocene soil

The Holocene soil overlays the uneven, wavy erosive surface of the described lithological units: Lithotamnian limestone, "residual clay", gravels, sand and silt of the Globoko formation, and is developed along the whole length of the trench. In the WSW direction up to 13 m where inclination of relief is steeper (app. 20°) the soil is thinner (10-20 cm) and is thickening to the ENE where the slope becomes more gentle (app. 5°-10°), and reaches the greatest thickness of nearly 1 m on a flat platform that has been occupied by the iron-age dwellings (Hallstatt culture, ca.500-800 years BC). The soil is dark yellowish brown (10YR4/2) silt with some organic matter (0.63 % TOT/C, samples L2/114, L2/115) and in average of 83 % silt, 8 % clay and 9 % sand and gravel (Appendix 5). It contains in average 42 % quartz, 7 % plagioclase, 4 % microcline, 31 % muscovite/illite, 14 % chlorite and 3 % goethite. The "pebbles" belong mostly to the Lithotamnian limestone, pottery ceramic or brick fragments, some other lithics and quartz. They are concentrated in the soil on a platform that has been occupied in iron-age and is most reworked by human activity (Fig. 21). Archeological findings from the soil horizon are described in two archeological reports (Appendices 2 and 3).

Apart from the fact that the interface between the Holocene soil and the underlying (Pl,Q) silt is being uneven, an important piece of observation is also that the soil appears to be infiltrated into the fissures in the strata below; even more so when we notice that the infiltrations are most prominent in (above) the fault zones (Fig. 22).

An analysis of the distribution of the total carbon (TOT/C) content in these joints infills (and in Pl,Q silt, in soil and "residual clay") was performed (Appendix 5). The equal TOC % in the very-superficial part of cracks (0 to 15 cm below the interface) and Holocene soil validated the interpretation based on macroscopic observation, stating that the "superficial V-shape cracks" of the fault-zone 2 are probably caused by a re-opening of pre-existing fractures where Holocene soil has fallen inside. The results of this analysis show also that infiltration is not limited only to the upper part of the faults but reaches app. 1,5 m in depth. The high correlation Pearson coefficient (0.88) between TOT/C content in the joints infill and the depth under the soil-sediment interface supports the hypothesis of contamination of some soil material into joints infill at depth (Figs. 22, 36, 37).

Possible interpretations of this phenomenon are described in the section *Deformation pattern and tectonic interpretation.*

Fig. 21. Limestone fragments are concentrated in the Holocene soil on a flat platform that has been occupied by the iron-age houses and are most probably reworked by human activity. The NE wall of the trench, between app. 21-24 m.

Fig. 22. Infiltration of "black" soil at the top of the trench section, in continuation of faults and fractures (red arrows) in the FZ1 area. Propagation of faults in the "brown silts" up to the Holocene soil interface with soil infiltration is shown vertical section and cleaned horizontal section at the modern soil interface is also shown.

Sedimentological interpretation of the Holocene soil. This unit of blackish clayey silt lies above the brown silts due to an erosion interface, which is in direct relation with the current morphology, and is thus attributed to the Holocene. The soil is composed of organic matter, clay and a few scattered elements (lithics, Badenian limestone fragments, pottery, brick fragments, etc). The interface with the lower (Pl,Q) silt is clearly strongly reworked by human activity (mix of upper organic soil and lower silty pseudogley horizons), especially where the two stone houses were excavated. Holocene soil and its basal interface are not deformed. The soil infiltration into the underlying silt unit is discussed in section Deformation pattern and tectonic interpretation.

3.2.3 Age dating of sediments

3.2.3.1 Overview and the results

13 samples altogether were selected for absolute age dating of which only 7 were successfully dated. 2 samples (of 5 sent) were dated by ^{14}C at Beta analytic (Appendix 6) and 5 samples (of 6 sent) were dated by OSL by Frank Preusser, University of Bern and Stockholm University (Appendix 7). None of the ESR samples from trenches were dated since we learned after submission that the laboratory that promised the service has no sufficient capacity.

Samples from Trench 2 were appropriate for OSL dating and were datable. According to the laboratory report (Appendix 7) there is no major methodological doubts about reliability of results, especially for the sample L2/10 (Table 2). The age of the Plioquaternary sand is thus estimated by OSL roughly at around 130.000 - 140.000 years b.p.

The 2 samples dated by ^{14}C yielded expected results (Table 2). In the first case (L2/2) the age is out of the method range while the second sample (L2/1) was obviously a modern root and was dated as modern.

Beside the trench samples, we received a set of 3 ESR absolute dates (Appendix 8) of samples from the Globoko open pit (a typical Plioquaternary fluvial succession along with one ESR date from the Plioquaternary sand taken from the borehole ES-1 (Bavec, ed., 2010) at a depth of 58,70-58,90 m (Table 2) at the time of reporting. Given the hypothesis that the sediments of our main concern in the Trench 2 belong to the same Plioquaternary Globoko formation, we use these results as valid also for the age determination of the Trench 2 sediment at this stage. The age for samples G 4-2, ES 1-3 and G 8-2 that were evaluated by the laboratory as more reliable (Appendix 8) is around 200.000 years b.p.. The ESR dating was done by Pierre Voinchet, Muséum national d'Histoire naturelle, Paris.

Sample	material	site	location of sample	OSL age (ka b.p.)	
				Quartz	Feldspar
L2/10	sand	Trench 2	PlQ sand layer; 2 m below surface	140 ± 14	134 ± 11
L2/12	silt	Trench 2	»PlQ overbank«; 1,7 m below surface	> 80	139 ± 11
L2/101	silt	Trench 2	»PlQ overbank«; 60 cm below surface	> 80	--
L2/102	silt	Trench 2	»PlQ overbank«; 2,7 m below surface	> 80	--
L2/103	silt	Trench 2	»PlQ overbank«; 70 cm below surface	> 80	--

Sample	material	site	location of sample	ESR age (ka b.p.)
G 4-2	silty sand	Globoko pit	»PlQ overbank«11 m below surface	190 ± 28
ES 1-3	sand	ES-1 borehole	»PlQ overbank«1.85 m below surface	204 ± 31
G 11	silty sand	Globoko pit	»PlQ overbank«5 m below surface	540 ± 81 *
G 8-2	sand	Globoko pit	»PlQ sand«7 m below surface	211 ± 32

Sample	material	site	location of sample	^{14}C age (ka b.p.)
L2/1	charcoal	Trench 2	»PlQ overbank«1.65 m below surface	recent
L2/2	charcoal	Trench 2	»PlQ overbank«1.85 m below surface	over 43ka
L2/3	charcoal	Trench 2	»PlQ overbank«2,30 m below surface	not datable
L2/105	charcoal	Trench 2	»PlQ overbank«1.10 m below surface	not datable
L2/106	charcoal	Trench 2	»PlQ overbank«0,75 m below surface	not datable

*Evaluated by the laboratory as less reliable

Table 2. Age dates from, or related to trench 2 at Libna. Top: OSL dates from trench 2. Middle: ESR dates from the Plioquaternary fluvial succession t the Globoko mine open pit. Bottom: 14C dates from trench 2.

The results are not consistent with understanding (including published works) of the age of the Plioquaternary sediments as it was interpreted prior to this project. There are evidences that do not converge with Globoko formation being as young as shown by the current absolute age, but all are non-conclusive:

- The pebbles are heavily weathered compared to any other known Quaternary aloformation in the region.
- Bulk lithologic composition does not resemble any known modern or Quaternary sedimentary hinterland. Namely, in the Pleistocene and Holocene Sava gravels, the carbonate pebbles account for 60 to 95 % of the sedimentary mass, whereas in the Plioquaternary the carbonate pebbles are not present at all. The non-carbonate content of the Quaternary (Sava River deposits) is identical to the Plioquaternary.
- The Plioquaternary sediments can be found up to app. 440 m (e.g. Premru, 1983) above the present course of the Sava River – the most probable transport media of the Plioquaternary sediments. On the other hand any Quaternary gravel aloformation can be only found as high as 120 m above Sava (e.g. Grad & Ferjančič, 1974) and even this only at the Alpine foothills where vertical displacements are known to be highest in Slovenia (e.g. Rižnar et al., 2005).
- Production of the carbonate pebbles/gravel in upper Sava river is known to be at least 284 ±32 ka old (Bavec et al., 2008), and ever since the sediment is lithologically identical (cf. Verbič, 2004). Hence the Pl,Q pebbles/gravel should be older.
- In Krško basin, the relief of the Globoko formation is significant. Verbič 2004 reports most extreme values at 250 m between the upper aloformation boundaries on Libna and in Borehole Mi-2, and as much as 350 m at its lower boundaries. As the borehole log may be incomplete we prefer using the tilt of the exposed lower boundary of the formation for relative comparison. It is estimated by field mapping at up to 8° at both flanks of the Krško syncline.

The age of Plioquaternary sediments/ Globoko aloformation is thus further discussed in section 3.2.3.2 below.

3.2.3.2 Discussion on the dating of the Plioquaternary sediments

The ESR and OSL age-dating within this project for the Globoko formation ("PlQ gravel") yielded ages at the range of roughly 130 – 210 ka b.p., which was very much unexpected. Finally, and with respect to what was previously published, we suggest 3 alternatives for the PlQ age estimation:

- The "**absolute age date option**", following the ESR OSL dates (see above) and the possible synchronicity of the artifact in the silty part of the formation, placing the age of formation at **130 – 210 ka b.p.**. Caution: there are some methodological limits to the used methods (ESR, OSL, see below), and some alternatives to explain the location of the artefact, explaining that it is not in a "depositional" (original) position (see section 3.2.4).
- The **"modeled option"** based on modeled extrapolation of the fluvial aloformations' geometry in Krško basin back in time. The modeled ages span **between 620 ka and 3 Ma**. Caution: this estimate is rough and based on many assumptions (see below).
- The **"published option"**, following the previous publications. We approximate the age of PlQ deposits based on previous published data at **around 2 Ma.** Caution: this estimate is based on approximation and on certain unverifiable stratigraphic assumptions (see below).

Up to now, we consider not to have enough conclusive arguments to favour any of these 3 options. An extensive and multi-method campaign of datings is required to conclude as there is no known single absolute dating method that would guarantee reliable age dating of the deformed sediments in trench on Libna and consequently the age of deformation.

1) The "absolute age date option"

Regardless of the doubts and a relatively large age-span when the two combined, we should be aware of the fact that the results of ESR (**around 200.000 years b.p.**; Globoko) and OSL (**around 130.000 - 140.000 years b.p.**; Libna, Trench 2) coincide well. In fact, they coincide extremely well, taken that by now we have been estimating the age of Plioquaternary with a precision at the order of magnitude of millions of years. In addition, we have to note again, that laboratories in both cases did not report any processing doubts even after a thorough in-person discussion (with OSL lab). However, in spite of luminescence dating being more and more widely used, one should be well aware of the fact that it is still an experimental method. The method is still being developed in its basic constituents and there are still numerous examples of severe errors in age determination. Generally, when problems have been reported, the ages are underestimated especially at ages higher than 70 ka (e.g. Lai, 2010; Lowick & Preusser, 2010; Lowick et al., 2010a; Lowick et al., 2010b). Even more so it is true for ESR, but we used all that is available at the moment. Cosmogenic dating may be the only remaining option but is also related with unacceptable amount of uncertainty at investigated locations.

Important outcome of this dating is that if these ages are correct, it will be easy to re-check them by a series of OSL dates from the Globoko pit at anytime in the future.

2) The "modeled option"

To independently test the diverging age estimates, we modeled the age of PlQ by using presumption of quasi-continuous deformation pattern from the beginning of deposition of Globoko formation until recent. Results are variable but still consistent enough to argue against the very young ages given by OSL and ESR. Definitions and absolute age-dates of aloformations are taken from work of Verbič (2004).

Elevation of upper surface. A diagram is constructed with the aloformations' upper topographic surfaces max. elevation in the Krško Basin, plotted against the age of the gravels. Vrbina aloformation (age=0; max. elev.:155 m), Drnovo aloformation (16 – 18 ka; max. elev.:160 m) and Brežice aloformation (117-145 ka; max. elev.:185 m) were taken into account. Their elevation vs. age

plots were extrapolated to the elevation of the Globoko aloformation (Pl,Q age ?; max elev.:350 m). It must be stressed, that 1) The assessment by the extrapolation considers not only tectonic uplift, but the sum of all processes involved (tectonics, sedimentation, erosion diagenesis, subsidence) which is true for all the gravels considered in the study, 2) Assumption is made based on elevation of northernmost exposure of PlQ lower boundary that the vertical movement is uniform at the scale of the study and that there is no differential block movements, 3) Input age dates are a rough estimate of various absolute age dates as approximated by Verbič (2004), 4) If results of the still developing luminescence dating are doubtful today, it even more so applies for the results that date nearly 10 years in the past. For the latter reasons alone this age estimates can be taken in the sense of estimation the order of magnitude and not as real brackets of age span. Different combinations of the extrapolated data gave the Pl,Q age **between 624 and 983 ka** (Fig. 23).

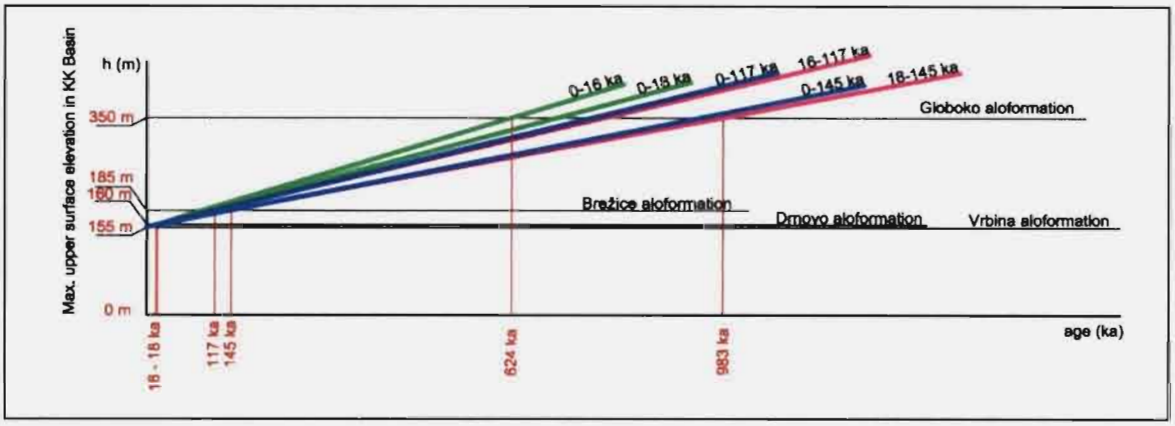

Fig. 23. Age estimation of the Globoko aloformation (Pl,Q gravel) based on extrapolation of the max. elevation of the Q and Pl,Q gravels. Input age dates are a rough estimate of various absolute age dates as approximated by Verbič (2004).

Tilt of aloformation. The Vrbina, and Drnovo aloformations are horizontal (not tectonically inclined) in the KK basin. The Brežice aloformation upper surface (117-145 ka) is tilted towards the KK syncline axis. Verbič (1995; 2004; 2005) reported the inclination of the upper surface of the Brežice aloformation on the Brežice terrace in the southern flank of the Krško syncline at 0,38°. In the northern flank of the syncline, the upper surface of the Brežice aloformation between Dolenja vas and KK-1 borehole is inclined 185 mrad or 1,060° (Verbič, 1995). The base of Pl,Q on the other hand is tilted up to 8° to the axis of the Krško syncline in both flanks. The modeled age obtained by this method ranges from **883 ka to 3Ma** (Fig. 24) and is driven also by assumption that upper and lower surfaces of each aloformation are parallel.

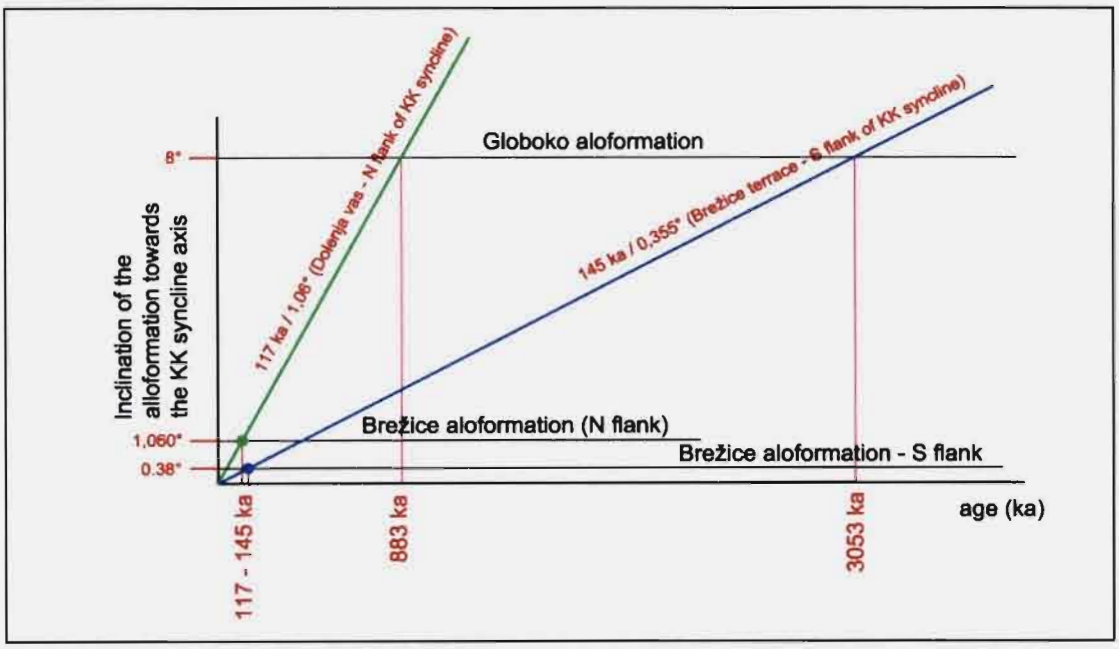

Fig. 24. Age estimation of the Pl,Q based on extrapolation of the max. inclination of the Q and Pl,Q gravels.

3) The "published option"

Before this study, we had no reliable absolute age dates available from the Plioquaternary succession in Slovenia nor were we aware of any comparative age date from the region. In the year 2000, the TL dating of the Plioquaternary sediments from the Globoko open pit (Bavec, 2000) gave the first estimate of absolute age by now. The minimum age of sediment was estimated at 306.000 years ± 2σ. It has to be stressed that this estimate was largely driven by the capability of the dating method in the year 2000 (very early stages of the luminescence dating on sediments). Thus this result was used only as the estimate of minimum age by now and by no means the estimate of age. In our Geology report (Bavec, ed., 2010) we used the Verbič's (2004) estimate where the Plioquaternary is estimated to 1 - 2 Ma, which is an estimate that is widely used based on convergence of the following indirect evidence.

By now, the age of the PlQ succession of the Globoko Plioquaternary aloformation was bracketed by its stratigraphic position between the youngest underlying Miocene (Pontian) formation and the oldest known overlaying Mid-Pleistocene gravel of the Brežice aloformation (e.g. Verbič, 2004). The youngest underlying Miocene silt was dated at Upper Pontian (after Piller et al., 2007; i.e. Upper Pannonian after newer divisions; discussed in the Geology report: Bavec, ed., 2010; pg. 163), which date to app. 5.5 Ma b.p., and the oldest overlying fluvial aloformation that was dated by Verbič (2004) at 117 and 145 ka, respectively. As Verbič's dates also rely on luminescence dating, the remarks noted above in the "absolute age date option" (see above) apply also here. In addition one has to note that direct superposition of the Brežice aloformation over the Globoko Plioquaternary aloformation was never directly observed in field.

Authors of the Basic geological map (Šikić et al., 1979) state that this PlQ succession is synchronous with the "Upper Paludina Beds", based on spatial relations and paleontological evidence. The dating then was done on paleontological inventory in the vicinity of Zagreb so we can not relate it to Krško basin with absolute certainty. Nevertheless, the spatial relation of the "Paludina lake" toward the SE with the Globoko formation as the remnant of the river that was feeding it, fits well. This would also

put the age of the Globoko formation very roughly (!) to at least around 2 Ma (Levantian → Villafranchian → transition of Pliocene to Pleistocene; Šikić et al., 1979; Rakić et al., 2002), which is also our estimate for the "published option" as whole.

3.2.4 Deformation pattern in Trench 2 and tectonic interpretation

Three structural blocks are separated by 2 main fault zones in the Trench 2 (Fig. 6). In the western side of the Trench, the fault zone 1 (FZ1) separates the Lithotamnian limestone of Badenian age and its "residual clay" from the major mass of the brown Plioquaternary silts (Fig. 5) that stratigraphically lie above the Plioquaternary gravel and sand (Pl,Q). To the east, the brown silts are in tectonic contact with the gravel and sand (fault zone 2, FZ2). The section is topped by a modern soil layer (including an archeological layer) which seems non-deformed by the post-Plioquaternary faults. Individual fractures are generally sub-vertical, and their strike is extremely variable. In very general, the strike of fractures varies around the general strike of the Libna Fault (mostly between N130° – N 170°) and around N230° which could be interpreted in the sense of Riedel system of the fault zone in NW-SE direction. The network of secondary structures along with the main ones produce a wide anastomozing zone of deformation (Fig. 25.) that probably extends further in the unexcavated parts. As mentioned by Lienkaemper and Williams (2007), multiple fault traces close to the surface and complex branching pattern leading to an anastomosing geometry are common features associated with coseismic ruptures of a recurrent character. This may also be due to the effect of the "free surface" during fault propagation.

Two alternative interpretations of what caused deformation observed in trench 2 were discussed during the survey: 1) the karstic collapse and 2) slope movement (such as landslide). The following observations speak against these alternative interpretations:

- The general deformation pattern is consistent and coincides well with the interpreted oblique dextral strike slip movement along a fault plane in NW-SE direction (the strike direction of Libna fault).
- The orientation of striae is also consistent and also coincides with the fault strike.
- All observation is consistent with predominant horizontal displacement as opposite to vertical displacement due to karstic collapse that was observed in trench 3.
- In the direction parallel to prevailing deformation pattern, the trench is situated at the very crest of the hill so interpretation of displacement in the direction of observed planes due to landslide seems to be less probable also from geomorphic perspective. On the other hand, in direction perpendicular to prevailing deformation pattern the trench lays on a significant slope. In spite that, there is no sliding planes developed indicating significant slope movement in that direction.

Fig. 25. Trench floor in the fault zone 2 (FZ 2) showing the tectonic contact between Pl,Q gravel (upper part of the picture) and the Pl,Q silt (lower part). Note the anastomozing pattern of the deformation. A view to ENE.

The Badenian limestone is affected by shearing. In the overlying "residual clay" the deformation is not visible.

The Plioquaternary gravel and sand unit is dissected by vertical fractures and faults. In the eastern side of the Trench, bedding tends to be horizontal, but it is substantially tilted to the west close to FZ2, against the brown silts. We notice a clear progressive unconformity inside the unit (see Fig. 11), for instance very clear between the basal Unit 1 with sand layers and the topmost unit 4 and further up against the overlaying silt which includes some rare bedding. This unconformity can correspond to a sedimentary structure because it is a common feature observed in high-energy continental deposits, and especially in the Globoko formation. Notwithstanding this hypothesis, its collocation with one of the main fault zone and with bed dips increasing faultward is an outstanding fact that may suggest also a genetic link to faulting.

The Plioquaternary silt is also tectonically deformed. The structural deformation pattern progresses upward from the Pl,Q gravel and sand into the silt without a notable change. Horizontal or gently dipping horizontal striations (0° to 30°) are recognized on several fault planes within the Pl,Q sediments (Fig. 26), clearly supporting our interpretation of this, being a strike slip fault (with a non-negligible vertical component) and proving the fault activity after deposition of the (Pl,Q) silt.

Fig. 26. Horizontal and gently dipping striations are found within the Plioquaternary succession (fault plane : N135, 55°E, striae plunge : 37°S; dextral)

A man-made silex artifact was discovered, included in the uppermost part of the Pl,Q silt unit and the silty matrix drapes it (Fig. 20). According to the archeological expertise (Appendix 3), the artifact is dated to between Mousterien (300.000 to 20.000 years b.c.) and the Neolithic (2.500 b.c.). As the Pl,Q silt unit is definitely faulted, two important questions arise from that: how old is the artifact, and when was it deposited to the current location (how and when did it get there)? It is positioned within the main tectonic zone (FZ1) 80 cm below the archeological surface, meaning it could be there due to late (Mousterien or later) transportation by tectonic displacement.

Several other interpretations of position of artifact within the PlQ fluvial silt were discussed:

- the human activity that produced the silex artefact is isochronous with the silt (either this formation is colluvial or fluvial), (also in Appendices 1 and 3)
- bioturbation may be the cause of a deep infiltration (also in Appendix 3),
- human activity isochronous with deposition of the (uppermost) silt (also in Appendix 2a)
- infiltration into desiccation or slope movement-related cracks,
- artifact was dragged down from surface by excavator during trenching.

The external expert D. Pantosti interprets that either the tool is in its initial depositional location, or it has been dragged down by event(s) related to faulting (then tectonic displacement is post-Mousterien, and in accordance with absolute datings implications).

The Holocene soil does not exhibit any clear sign of tectonic deformation and the interface with the underlying silt is not displaced. This observation is both geological as well as archeological (Appendix 3).

Yet again, there are several observations that may also lead to a conclusion that the fault at this site has experienced tectonic displacement after (or during) the area was inhabited during the Hallstatt, ca. 500-800 years BC.

The Holocene / pre-Holocene interface has a mean slope of 23%, from 30% in the first 13 upslope meters, to 14% in the last 7 down-slope meters. Along the interface of the Holocene soil with the underlying silt, a "large-wavelength" kink that disturbs the regular decrease in slope is observed. Two flat platforms (one in each side of the trench) have been occupied by the Hallstatt houses where the interface is clearly strongly reworked by human activity (mix of upper organic soil and lower silty

pseudogley packages). Although the soil and its basal interface are clearly not as deformed as the underlying silts and conglomerates, it was noticed (also by the external expert D. Pantosti) that:

1. The interface slope is disturbed at the exact location of FZ2. This disturbance can effectively be due to human activity during the iron-age. However, D. Pantosti remarked during her visit that this kind of feature (occupation of natural coseismic terraces by humans) is a common feature along active faults in Italy. As we do not have any idea of the amount of iron-age digging (i.e. deformation of natural relief), we cannot conclude anything with this.

2. Another interesting observation is the local infilling of the soil into faults at the interface of the soil and the Pl,Q silts. This was visible in vertical sections and corroborated by horizontal cleaning during the last re-visit of the Trench (Fig. 22). The most prominent feature of this kind was found directly above one of the main faults of the FZ2. Such prominent infiltrations were not observed elsewhere in the Trench 2 and in the Trench 3, at the base of the modern soil and colluvium, and Holocene coseismic activity of faults was then suspected (including by D. Pantosti).

Superficial infiltration of Holocene soil into open surface fractures can be interpreted as infiltration of Holocene soil into the open surface fractures. Surface fissuring (then fissure fills in geological record) in the close area of active faults is a classical feature of coeval tectonic displacement. It is even often associated with coseismic events because it corresponds to rapid brittle failure of soil. This has been largely documented by numerous earthquake geology surveys all over the world, for the past and the recent events, whatever the tectonic regime:

- Especially in extensional regime (e.g. McCalpin 2005).
- Also in compressive regime: tensile cracks of fault-propagation anticlines on the hanging-wall (e.g. Meghraoui & Doumaz, 1996; Lee et al., 2004) or fissures in the collapsed area of the hanging-wall, behind active thrust (e.g. Philip et al., 1992).
- And in oblique (tensile fissures along pressure ridges: e.g. Philip et al., 1992) or pure strike-slip environments (fissures directly associated with faults: e.g. Lienkaemper et al, 2002; Lienkaemper & Williams, 2007). These last authors even consider fissure fillings as a feature unique to coseismic displacement (excluding creeping), whereas more ambiguity is left about possibilities for discriminating among creep and coseismic deformation in latter work of Lienkaemper et al. (2011).

As mentioned above, coseismic open cracks are commonly observed along (or close to) the source fault: they are also, but more rarely, found in the far-field area (then often associated with secondary effects such as liquefaction, gravity sliding). Moreover, the presence of such open cracks in trench 2 – if they really exist- near the soil base, not erased by the pre-archeological erosion period (i.e. during glacial period) would indicate that the observed deformations are quite young (post glacial period).

At least two "non-seismic" interpretations of V-shaped cracks genesis have also been discussed during trench survey:

- Opening of cracks due to mass movement (the modern surface is inclined at about 10°)
- Desiccation is the controlling process.

The problem of discriminating between tectonically induced infiltrations and non-tectonic ones is also pointed out in work done by Lienkaemper et al. (2011) on the Green valley fault, where (in cases

similar to ones found in trench 2) the authors hesitated in discriminating between the tectonic and non-tectonic origin of fissure infills and sand-filled cracks.

Infiltration of modern soil solely in the upper part of faults may thus be an evidence of fault opening during a tectonic event (along Libna fault or along an associated fault like Orlica and Artiče faults), during Holocene. To support this interpretation the analysis of the distribution of the total carbon (TOT/C) content in the Pl,Q silt, soil, "residual clay", and joints infill was performed (Appendix 5). The result was sought through corroboration of these results with other analytical results (described above) yet no conclusive result was obtained, except for the fact that infiltration is not limited only to the upper part of the faults but reaches app. 1,5 in depth. The high correlation Pearson coefficient (0.88) between TOT/C content in the joints infill and the depth under the soil-sediment interface supports the hypothesis of infiltration of some soil material into joints infill (Figs. 22, 40, 41).

Field observations show that the material in joints infill is softer; less compacted and could consequently be more porous and permeable than the surrounding sediment. Lowered Eh due to percolating water caused color changes in the neighboring sediment (Fig. 37). From that we conclude that water percolates preferably along joints and the increased TOT/C content may also origin form purely "non-tectonic" processes. It is also seen that modern plant roots in both trenches preferably follow the joints (Fig. 18, 19, 37) as they prefer softer joint infill material to harder surrounding sediment (not exclusively, though). The root bioturbation made joints progressively more permeable. However, in conclusion we can say that this analysis cannot prove or reject the hypothesis on infiltration of the modern soil in the uppermost part of the joins (faults) caused by opening during Holocene tectonic/seismic event.

3.2.5 Evaluation of displacement along the Libna fault from findings in and near trench 2

Displacement along the NE branch of the fault (FZ 2) is assessed from observations in the Trench and supported by additional geophysical interpretation (Appendix 4) to be at the order of magnitude of several meters (less than 10 m in the horizontal direction) (Fig. 27). From the trench log it is interpreted that the main branch may be the SW (FZ 1) and from the regional geophysics we may suspect that there may be even more deformation accumulated along the whole width of the Libna fault outside the two fault zones mentioned here. Then, Trench 2 alone does not allow estimating the total displacement associated to this fault.

According to the current tectonic model (Bavec, ed., 2010), the potential displacement is not distributed evenly along the whole length of the Libna fault. It is supposed to be concentrated mostly to differential folding along the Libna fault thus and most deformation should be taken up on the Libna anticline.

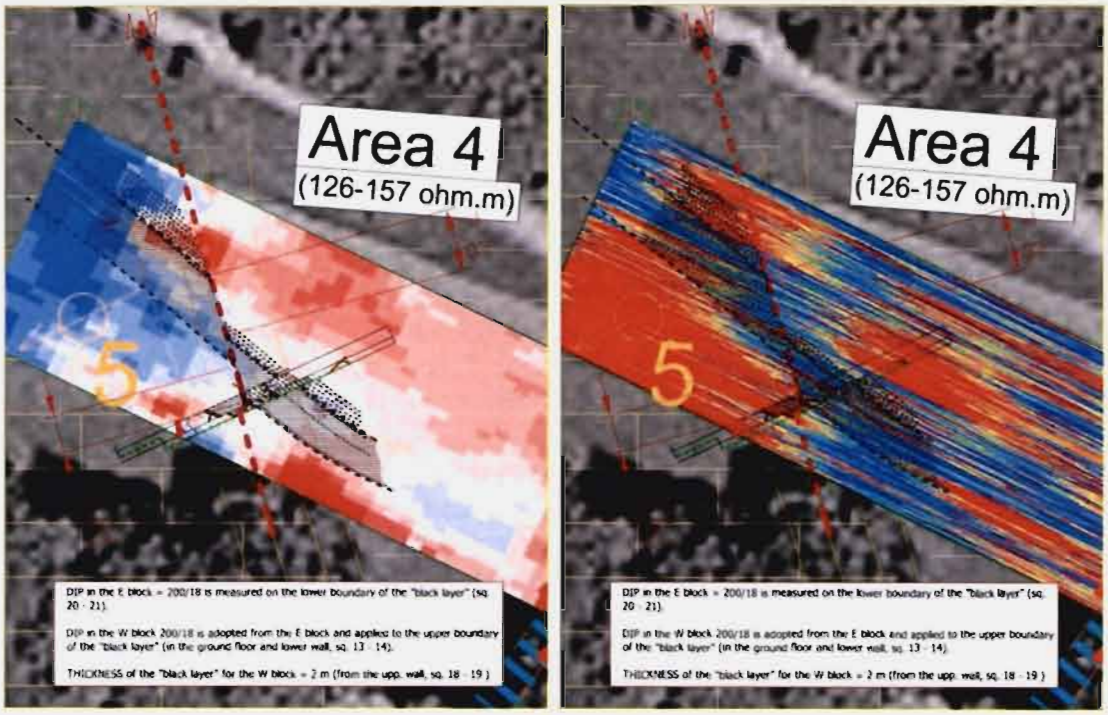

Fig. 27. Displacement estimate along the FZ2 is based on dip and thickness of the layers in the trench, and the combination of GPR and electric resistivity survey of the nearby area.

3.3 TRENCH 3

3.3.1 General overview of findings in trench 3

Trench 3 was excavated into the Lithotamnian limestone of the Badenian age, "residual clay" (Fig. 28), and brown silt with thin gravel beds of the Plioquaternary age. The residual "clay" is covered by brown silt with small quartz and some lithic pebbles that is topped by modern soil that covers brown silt of the Plioquaternary age also. The "residual clay" is cut by small fractures dipping mostly in the NE direction. Between 11 m and 16.5 m, small displacements of minor blocks along the fractures can be seen. The fractures (or faults) do not propagate into the overlying succession of Plioquaternary silt nor into the topmost colluvial unit and soil. No infiltration of topmost soil into the underlying sediment was observed.

The fractures cutting the "residual clay" and small displacements along them are most probably caused by nearby tectonic movements detected in the Trench 2 or by local karstic collapse. As the deformation pattern does not propagate into the Plioquaternary succession above, we infer that the deformation observed in trench 3 is post-Badenian and pre-Plioquaternary.

Fig. 28. The view of the Trench 3 in the NE direction. In front the Lithotamnian limestone of the Badenian age covered by the "residual clay".

The NE wall of the Trench 3 was logged in detail, while opposite wall was used for gathering additional information. Floor and the "step" (created to enable stability of wall) of the trench were also logged (Fig. 29).

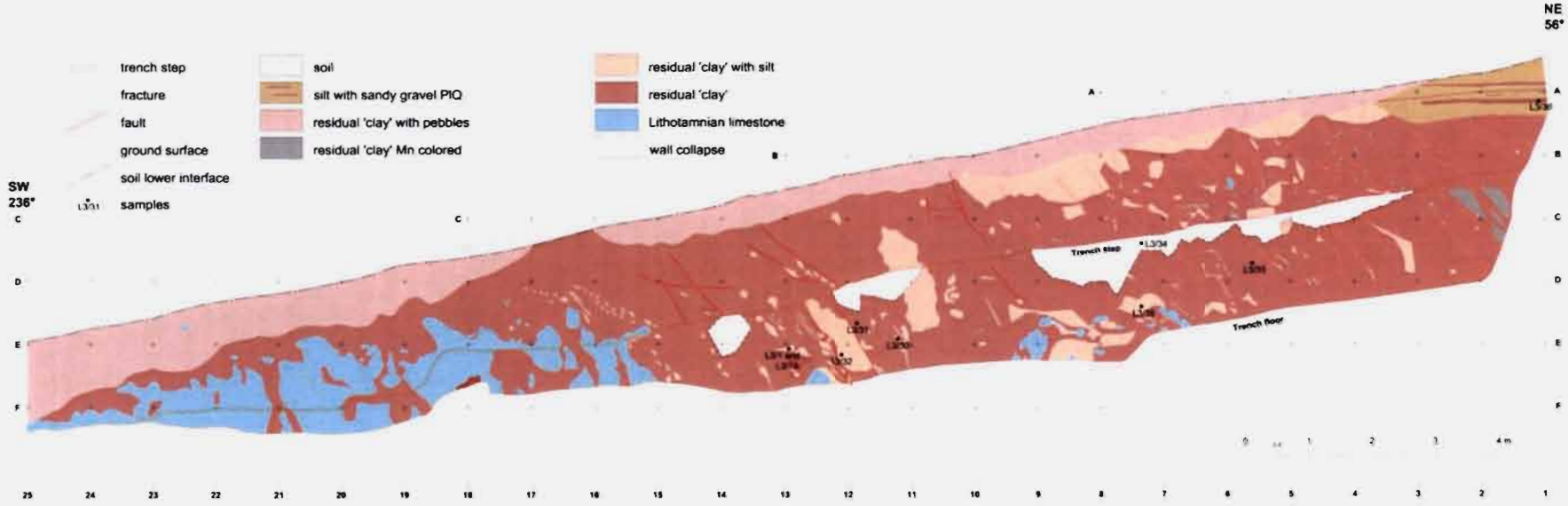

Fig. 29. The log of trench 3.

3.3.2 Description and interpretation of main sedimentary units

3.3.2.1 The Lithotamnian limestone - Badenian

The Lithotamnian limestone of the Badenian age crops out mostly in the SW part of the Trench 3 and is covered by the "residual clay". The Lithotamnian limestone was examined only macroscopically. It is white, has bindstone and calcarenite structure and among other fossils, contains mostly fragments of bivalves, bryozoans and foraminifers encrusted by rhodolites forming red algae (Lithotamnian) (Fig. 30). The Lithotamnian limestone is massive, fractured, weathered and intensively karstified in the upper contact with the "residual clay", forming very uneven, corroded surface with up to 80 cm deep indentations filled by "residual clay". Isolated fragments of very fractured and corroded limestone are found in the "residual clay" (Fig. 31) (Fig. 32).

Fig.30 The Lithotamnian limestone – bindstone

Fig. 31. Intensively karstified Badenian limestone, forming very uneven, corroded surface indentations filled by the "residual clay". The NE wall of the trench, 14-22m.

Fig. 32 Intensively fractured block of limestone in the "residual clay".

3.3.2.2 The "residual clay"

The "residual clay" lays on the karstified surface of the Badenian Lithotamnian limestone and is overlaid mostly by up to 1.7 m thick brown silt with small pebbles. The light brown (5YR5/6) "residual clay" is mostly massive, somewhere laminated. The laminas are discontinuous, limited in length, and marked by color differentiations caused by different FeO(OH) concentrations (Fig. 33) or silt laminas (Fig. 34). Silty patches (ghost sand clasts) of irregular shape and size are unevenly disposed in the "residual clay" (Fig. 35). Smaller silty patches are concentrated in the upper part of the "residual clay" under brown silt with small pebbles too. The "residual clay" is locally marmorised and contains dark grey patches, most probably colored by Mn oxides and hydroxides.

The "residual clay" consists on average of 79 % silt, 20 % clay and 1 % sand grain size fraction and has a main grain size of 0.013 mm. The "residual clay" should be named the residual silt according to these data. In order to distinguish it from the other lithologic units we refer to it as "residual clay". Mineralogical composition is: 17 % quartz, 2 % plagioclase, 43 % muscovite/illite, 13 % chlorite, 19 % kaolinite and 7 % goethite (Appendix 5). Muscovite is weathered to poorly crystallized illite.

The silty patches (ghost clasts) contain on average 67 % silt, 23 % sand, 10 % clay and are composed of 58 % quartz, 3 % plagioclase, 3 % microcline, 29 % muscovite/illite, 4 % chlorite, 1 % kaolinite, and 2 % goethite.

The "residual clay" is cut by a network of fractures dipping mostly in the NE direction. The "residual clay" is more pale or even grey (N7 – 5B7/1) (Fig. 36, 37) along the colored fractures. Modern roots follow the fractures in some places. Between 11 m and 16.5 m. Minor displacements of small blocks can be seen along the fractures (faults) (Fig. 33, 34). Small patches placed along the fractures are constituted by silt (Fig. 38) containing 90 % silt 3% sand.

Fig. 33. Laminas marked by color differentiations caused by different FeO(OH) concentrations are cut by fractures (faults) along which small blocks are displaced. The NE wall of the trench at 12.8 m.

Fig. 34. Part of the "residual clay" with silt laminas dissected and displaced along smaller fractures. The NE wall of the trench at 12.3 m.

Fig. 35. The silty patches – ghost clasts and weathered limestone in the "residual clay". The NE wall of the trench at 7.3 m.

Fig. 36. A net of differently sticking fractures along which the "residual clay" is more pale colored or even greenish grey. The fractures dip mostly to the NE. Step of the trench from 3 m to 4 m.

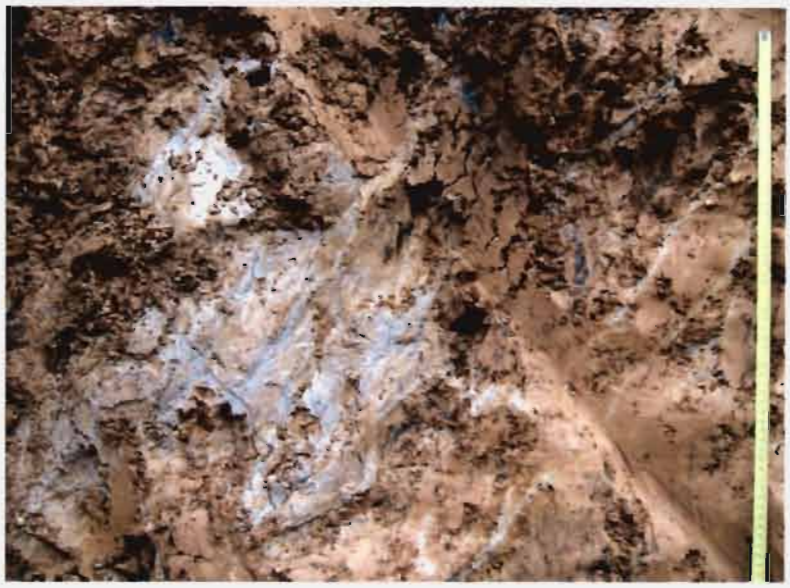

Fig. 37. Gray colored "residual clay" along the fractures with visible recent roots on the fracture plane and dark grey patches most probably colored by Mn oxides and hydroxides. The SW wall of the Trench 3 between 0.5 and 3 m.

Fig. 38. Cavities that formed along the fractures are filled by silt. NE wall of the Trench 2 at 11.6 m.

Interpretation: The "residual clay" is interpreted as paleosol – chromic (brown) cambisol developed on the Lithotamnian limestone during its exposure and before the deposition of the Plioquaternary sediments.

The fractures cutting the "residual clay" and small displacements along them are very probably caused by local karstic collapse or by nearby tectonic movements as detected in the Trench 2.

The color change of the "residual clay" along some fractures to paler brown or even grey color is caused by percolation of the water with lower Eh. This water was reduced after percolation through a modern soil rich in organic matter.

On the basis of the similarity of the mineralogical and chemical composition of some samples of the Plioquaternary (i.e. Globoko aloformation) sediments from the Trench 2 and samples of the ghost clasts and silty patches in the Trench 3 (discussed later), these are interpreted as infiltration/incorporation of the overlying Plioquaternary silts into the "residual clay". This happened after the disturbance caused by karstic collapse or possibly even by nearby tectonic movements detected in the trench 2.

3.3.2.3 The brown silt with thin beds of sandy fine gravel

A channel, filled by pale to moderate yellowish brown (10YR6/4) predominantly pebbly sandy silt and silt with three thin (2 to 10 cm thick) layers of pebbly fine sand to sandy fine gravel (Fig. 39) is cut in the underlying "residual clay" in the NE part of the Trench 2 between 0 and 4 m. The three layers pinch out in the SW direction. The pebbly sandy silt contains 10 to 25 % of pebbles more abundant in the upper part. The mean grain size is 3-4 mm but the pebbles may reach up to 20 mm in size. They belong to quartz and different reddish, grayish, some nearly blackish and greenish clastic sedimentary and volcanic rocks. No structural deformation was observed to propagate into this unit from the underlying "residual clay".

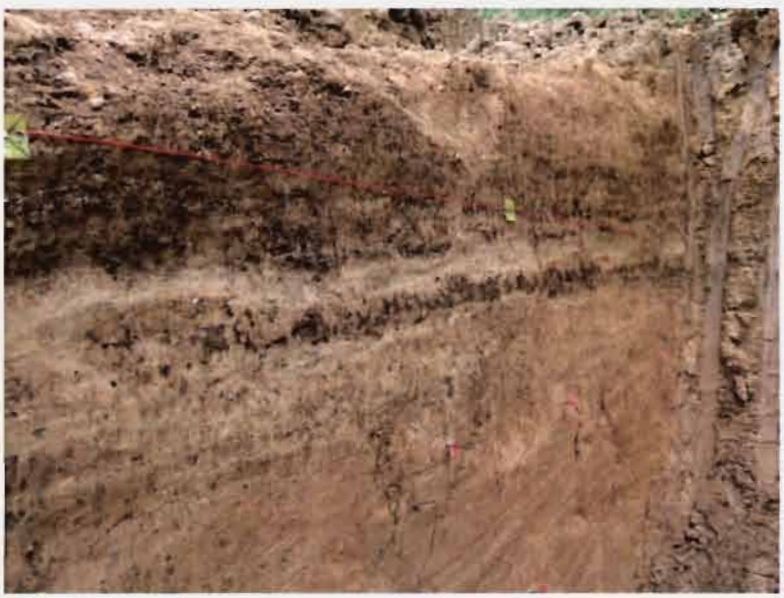

Fig. 39. A channel filled by yellowish brown predominantly pebbly sandy silt and silt with thin beds of pebbly fine sand to sandy fine gravel. The bottom of the channel is marked by violet flags. The NE wall of the trench between 0 and 3 m View to the NE.

The silt consists of 75 % silt, 17 % sand and 8 % clay grain size fraction and contains 45 % quartz, 4 % plagioclase, 6 % microcline, 30 % muscovite/illite, 13 % chlorite and 3 % goethite. The beds of pebbly fine sand to sandy fine gravel are darker, grayish brown (5YR3/2) and contain 20 to 50 % of pebbles of the same sizes and composition as in the pebbly sandy silt.

Interpretation: By checking surroundings of the trench we found outcrops of the Plioquaternary (i.e. Globoko aloFm) sediments a few meters above the upper level of the trench 3. According to this fact the infill of the erosive channel is interpreted as beginning of the deposition of the Plioquaternary sediments. This interpretation is also supported by cluster analysis of mineral composition and combination of mineral and chemical composition of all samples analyzed from the Trenches 2 and 3 (Appendix 5).

3.3.2.4 Brown silt with pebbles

The brown (5YR5/6) silt with pebbles is the same color as the underlying "residual clay" and has undulated lower contact .It is 0 to 1.2 m thick and is the thickest in the SW part of the trench 3.The brown silt is missing between 16 and 17 m. The silt with pebbles contains less than 5 % of pebbles, mainly 2-5 mm grain size that are represented mostly by quartz and less abundant other lithic pebbles. Their composition is very similar to the composition of the pebbles in the overlying Plioquaternary sediments. No structural deformation is observed in this unit.

Interpretation: The brown silt with small pebbles is interpreted as a colluvial deposit of the "residual clay" and of the overlying Plioquaternary sediments, mostly pebbles.

3.3.2.5 The modern soil

The modern soil covers the brown silt with small pebbles, the brown silt with thin beds of sandy fine gravel of the Plioquaternary age and (only in the length of one meter) the "residual clay". During the excavation of the Trench 3 it was removed for safety reasons (to avoid collapse) and will not be analyzed in more detail. No structural deformation is observed in this unit. The interface with the underlying sediment was thoroughly checked for possible downward infiltrations (such as observed in trench 2).

3.3.3 Structural observations

The "residual clay" is cut by a network of fractures dipping mostly in the NE direction but with a significant variability. The fractures are of limited extend and amount of displacement is rarely observable. However, some minor normal displacements (at the range of centimeters) of small blocks can be seen along some faults at the base of the section (Fig. 33, 34), along fault planes with changing dip angle (listric pattern sometimes). The general pattern of the section, with karstic caves at the base of a formation affected by faulting with a normal and sometimes "listric" pattern, suggest that gravitational displacements of karstic origin occurred there yet we cannot exclude possible relation to tectonic displacement observed in trench 2.

The silty patches (sand clasts) and silt infill of joints included within the "residual clay" mass are compositionally similar to some samples of PlQ gravel matrix or PlQ sand from the trench 2 and PlQ silt from trench3 (Appendix 5). This lead us to an interpretation that the silty patches (sand clasts) and silt infill of pores (joint) in the "residual clay" from the trench 3 are products of infiltration /inclusion of the overlying "Globoko" silts into the "residual clay", following subsidence beneath the trench floor by (endo)karstic phenomenon or possibly tectonic movement.

The fractures and faults do not propagate into the overlying succession of topmost colluvial unit and soil. No infiltration of topmost soil into the underlying sediment was observed. The deformation also does not propagate into the Plioquaternary succession above, thus we infer that the deformation observed in trench 3 is post-Badenian (significantly younger of Badenian as the deformed residual clay needed time to be formed) and pre-Plioquaternary.

3.4 Analysis of granulometric, mineralogical and chemical composition of sediments in Trenches 2 and 3

3.4.1 Overview of laboratory results and the statistical (cluster) analysis

After the initial interpretations some important questions arose regarding the composition and genesis of the materials observed. The main purpose of the grain size, mineral and chemical analyses was to characterize/discriminate of sedimentary units and to analyze the material of joints infill. All the details of these analyses are presented as appendix 5 to this report and only the overview and conclusions are presented here.

It has to be noted that the statistical analysis presented here can only be used as an aid and not as conclusive evidence. The number of analyzed samples may be relatively high for a usual paleoseismological trench but still low for a firm statistical analysis.

From the grain size data it can be concluded that most of the samples (34) are granulometricaly classified as silt, even those classified as residual clay (for readability the name "residual clay" is kept in this report) in the field. For the residual material of the Badenian limestone it is very unusual to contain so high portion of silt fraction. The presence of allochtonous, very probable aeolian maternal, as known in many soils of "terra rosa" in the Mediterranean region is suspected. Grain size distributions of the Pl,Q overbank silt and material of joints infill from the T2 are nearly identical, except for the sample of joint infill in FZ2, app. 2 m below surface (L2/27A) that is coarser grained (sandy). Beside the last mentioned sample, five more samples are coarser grained as well: samples L2/27A and L3/35 are classified as sandy silt; sample L2/10A as silty medium grained sand; samples L2/2SG, L2/M2 as muddy gravel and sample L2/M1 as gravely muddy sand.

By mineral composition the analyzed samples can be grouped into five clusters. The largest cluster 1 includes majority of samples of the Pl,Q silt, joints (faults) infill and soil. Only one reddish joint infill in the Pl,Q sand (Unit 4) is classified in the cluster 2 together with samples of "residual clay" and with the red tectonic lens from the T2. In the cluster 3, samples of "residual clay" are grouped including grey joint infill within "residual clay" from the T3. Samples of silty patches (sand clasts) in the "residual clay" from the T3 and a sample of the Pl,Q silt from the T2 are enclosed in cluster 4 while cluster 5 includes samples of gravel matrix, Pl,Q sand from the T2 and silty joint infill in the "residual clay" from the T3.

Very similar grouping of the samples characterized by combining mineral and chemical composition was achieved with solution of 7 clusters by k-mean cluster analysis. Two samples are outstanding and occupy their own clusters. The most outstanding is sample of joint infill L2/27A (cluster 4) and to a less degree a sample of Pl,Q sand L2/10A (cluster 6). Comparing grouping of samples based on mineral composition with grouping based on mineral and chemical composition combined, one can see that the chemical composition causes the difference. Chemical composition (mostly content of Ba and Th) discriminated in 7-cluster solution also between clusters 2 and 3, which are the most similar to each other of all. Cluster 2 encompasses mostly samples of joints (faults) infill and Pl,Q silts from the upper step of the T2 while samples from cluster 3 are taken from the Pl,Q silt from the lower step of the T2, and the Holocene soil. Higher content of Th in Cluster 2, and higher content of Ba in cluster 3 is observed. In the 4 and 6 k-mean solution both clusters are united (Appendix 5). The samples of joints (faults) infill from the T2 are not differentiated, but it is obvious that the L2/C3 sample (the reddish joint infill in the Pl,Q sand) differs from the others. The cluster 5 encloses samples of silty patches (sand clasts), silt infill of pores (joints), Pl,Q silt from the T3 and gravel matrix from the T2. It is interesting that in all cases of cluster analysis samples of silty patches (sand clasts) and silt infill of joints in the "residual clay" from the T3 are clustered with some samples of gravel

matrix or Pl,Q sand from the T2 and Pl,Q silt from T3 (Appendix 5). This leads us to an interpretation that the silty patches (sand clasts) and silt infill of pores (joint) in the "residual clay" from the T3 represent products of infiltration of the overlying Pl,Q silts into the "residual clay" after disturbance caused by nearby tectonic movements detected in the Trench 2. The silt laminas in the "residual clay" bounded by fractures may also be interpreted that way. Samples of "residual clay" from T2 and the ones from the reddish tectonic lens from the fault zone 1 form cluster 7. Samples of "residual clay" from the T3 with the grey joint infill are joined in cluster 1. Note that (L3/34Z) sample of grey joint infill is classified in the 4 and 5 cluster solution together with other samples of joints infill and Pl,Q silts from the upper step of the T2.

Possibility of the Holocene soil infiltration into some joints was tested at the IRSN laboratory by additionally analyzing total carbon (TC) and total organic carbon (TOC) in 21 samples. The depth under the soil-sediment interface (Depth), average (TOT/C) of (TC) analyzed by IRSN and (TOT_C) analyzed by ACME is given In the Table 4. Comparison of the data of TOT/C and TC from both laboratories detected significant difference in five of analyzed samples. Among others, differences were within the declared analytical error. TC and TOC chemical analysis showed that nearly all carbon is in fact organic carbon (TOC). This is also supported by the mineralogical analysis as no carbonate minerals were found within the analyzed samples.

The k-mean cluster analyses with solution of 7 clusters were run only on the chemical composition data analyzed by ACME. The analysis of variance shows that TOT/C is among 17 statistical non significant ($p<0.05$) variables. In other words, variances of TOT/C are larger within clusters then between clusters. It is also interesting that samples of the Holocene soil, the joints infill from the T2 just under the soil, and the grey joint infill (L3/34Z) in the "residual clay" from the T3 form their own cluster 1 (Table 3).

Sample	Lith./locat.	Cluster	Distance	Case_No
L2/112	joint	1	3,90	18
L2/113	joint	1	3,52	19
L2/114	soil	1	5,92	20
L2/115	soil	1	4,52	21
L2/116	joint	1	4,89	22
L3/34Z	joint	1	8,65	26
L2/26A	PIQ silt up	2	6,06	9
L2/C1	joint	2	5,85	10
L2/C3	joint	2	8,29	11
L2/C5	joint	2	5,00	12
L2/2SG	matrix	2	10,20	15
L3/30	joint	2	6,17	23
L3/36	PIQ silt	2	10,44	28
L2/20	PIQ silt low	3	4,76	5
L2/12A	PIQ silt low	3	5,96	6
L2/22A	PIQ silt low	3	3,36	7
L2/23A	PIQ silt up	3	5,93	8
L2/28A	PIQ silt low	3	3,85	14
L2/GMU	matrix	3	5,31	16
L2/104	PIQ silt up	3	7,27	17
L2/27A	joint	4	0,00	13
L2/10A	PIQ sand	5	10,71	1
L3/35	sand clast	5	10,71	27
L3/31	Resid_Bad	6	5,38	24
L3/34O	Resid_Bad	6	5,38	25
L2/15A	Resid_Bad	7	5,10	2
L2/16A	Resid_Bad	7	4,10	3
L2/18A	red tct lens	7	8,56	4

Table 3: Cluster members (samples) defined by chemical composition and their distances from the cluster centers

The samples from the T2 in the cluster 1 have also the highest concentrations of TOT/C of all analyzed samples. Higher concentration of TOT/C than the average for the PIQ silt is detected also in the reddish joints infill (samples: L2/C3, 105 cm below the modern soil; L2/C5, 225 cm below the modern soil). Plot of TOT/C versus depth was constructed for 24 analyzed samples (Fig. 40). The total carbon (TOT/C, which is mostly organic carbon) infiltration along the joins is supported by the scatter plots TOT/C versus Depth (Fig. 41) and high (0.88) correlation Pearson coefficient.

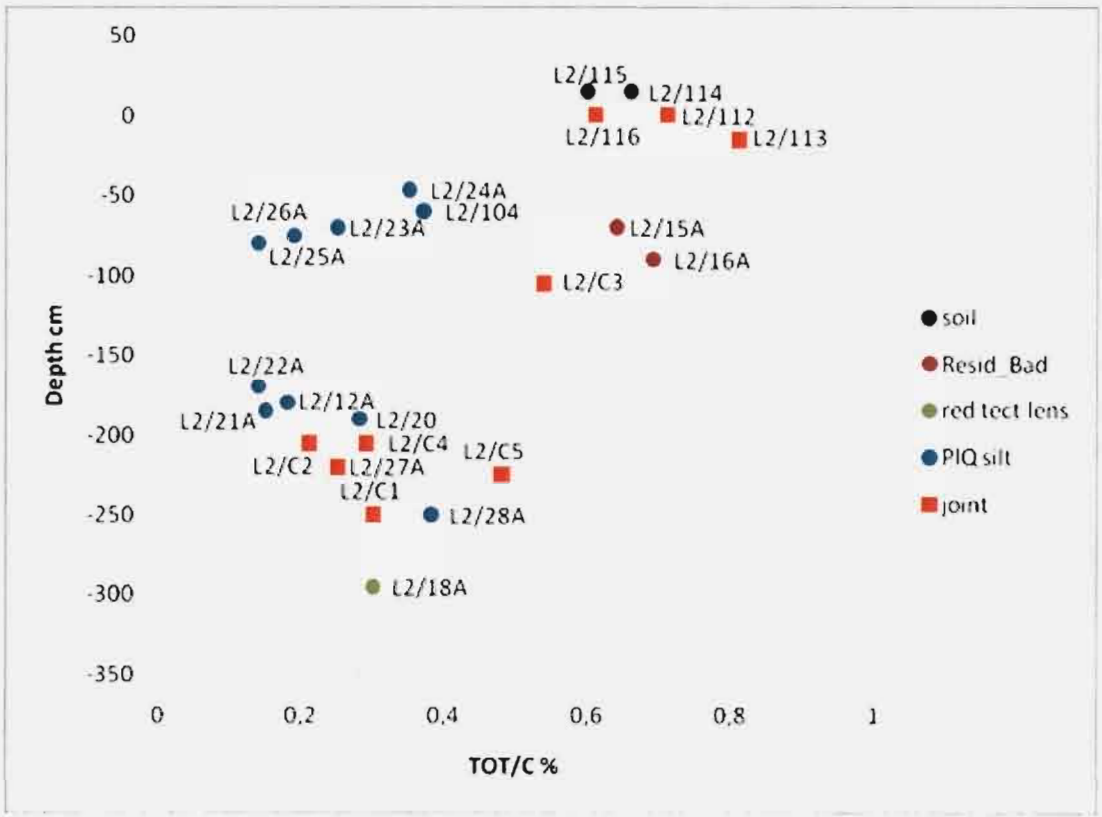

Fig. 40 Scatter plot of the TOT/C (%) content in the PIQ overbank silt, Holocene soil, "residual clay" and joints infill versus the depth below modern soil of the 24 analyzed samples.

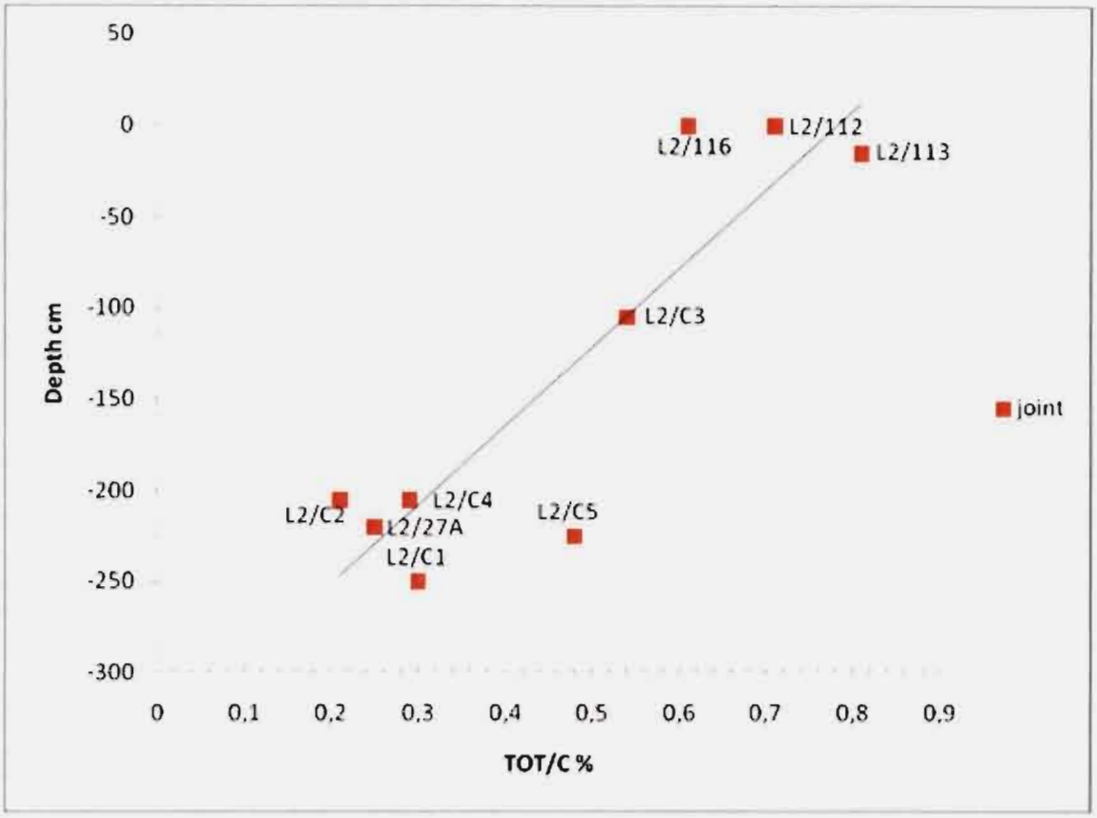

*Fig. 41 Scatter plot of the TOT/C (%) content in the joints infill versus the depth below modern soil of 9 analyzed samples and their correlation [Depth = -338,11+432,84*x].*

3.4.2 Conclusions from analyzing the mineralogical, granulometric and geochemical composition of sediments

Two hypotheses were discussed within the team over the genesis of the Pl,Q silt. One interpreted PlQ silt as an alluvial overbank flood plain sediment that was modified by pedogenic and other processes or as being of colluvial origin. On the basis of field observations we support the first hypothesis, but with laboratory analyses presented here we cannot prove or reject none of the two hypotheses.

The mineralogical and chemical composition of all the Pl,Q samples is in full correlation with the grain size of analyzed samples: gravel matrix groups together, sand groups together and silts groups together, respectively. However, two of the main questions asked in this analysis were: 1) is the silt colluvium and/or 2) is the silt differentiated into two parts, e.g. into lower overbank deposit, and overlying colluvial cover. In this respect we have to mention a slight differentiation among those silt samples that lay less than 1 m below the Holocene soil, and those that lay deeper. Namely in one of the cluster solutions of chemical analyses, differentiation among the two was identified based mostly on (small) differences in content of Ba and Th (see above and Appendix 5).

The silty patches (sand clasts) and silt infill of joints in the "residual clay" from the Trench 3 are compositionally similar to some samples of PlQ gravel matrix or Pl,Q sand from the Trench 2 and Pl,Q silt from the Trench 3.

Grain size distributions are nearly identical in the PlQ silt and in the silt in the joints infill, except for the (L2/27A) sample of joint infill from FZ 1, app. 2m below the modern soil that is coarser grained

(sandy). It is outstanding also in the mineralogical and chemical composition. However, most of the joints infill silt samples have nearly the same mineral composition as the PlQ silt, matrix of gravely silt and the Holocene soil. The mineralogical composition of the red tectonic lens (L2/17A, L2/18A) and joint infill (L2/C3) is closer to the "residual clay" of the Trench 2.

The mineralogical and chemical composition similarity between the PlQ silt and the Holocene soil is not surprising as the PlQ silt was obviously parent material for the soil.

Distribution of the total carbon (TOT/C) content in the PlQ silt, soil, "residual clay" and joints infill versus depth under the soil-sediment interface (Depth) and the scatter plot of the TOT/C content in the joints infill versus the depth under the soil-sediment interface were used to test the hypothesis of possibility of modern soil infiltration into some joints infill at depth (Fig. 41). The high correlation Pearson coefficient (0.88) between TOT/C content in the joints infill and the depth under the soil-sediment interface supports the hypothesis of infiltration of some soil material into joints infill. According to field observations, plant root bioturbation, and color changes it is obvious that water percolates along joints. After water percolate through soil its Eh is getting lower that influences the neighbor sediment (color changes), infiltration of some material from the soil above can be expected. However, this analysis cannot prove or reject the hypothesis on infiltration of modern soil in the uppermost part of the joins (faults) caused by opening during Holocene tectonic event.

The "residual clay" on the Badenian limestone mineralogicaly and chemically slightly differs among the trenches 2 and 3. The main difference is in the content of kaolinite. It is present only in the "residual clay" in the Trench 3.

The color of the "residual clay" changes from moderate brown to paler brown or even grey along joints. We interpret that this is caused by percolation of water with lower Eh along joints. This water was reduced after percolation through a modern soil. The mineralogical composition of these joints infill did not change and is very similar to the "residual clay", but some slight changes in chemical composition are observed.

It is unusual that the residual material of the Badenian limestone contains so large portion of silt fraction. We suspect the presence of allochtonous, very probable aeolian maternal, as it is known in many soils of "terra rossa" in the Mediterranean region.

4 POTENTIAL IMPLICATIONS OF NEW FINDINGS FOR SEISMIC HAZARD AND CAPABLE FAULT ISSUES

From observations on the Libna fault, the following issue arise that implies a need for further clarifications:

- The Libna fault may also be described as a capable fault and additional data and/or analysis are required because some important issues for the assessment of the potential impacts of the fault are still open. Should the Libna fault be considered a seismic source in seismic hazard assessment?

4.1 LIBNA FAULT AS A CAPABLE FAULT

Libna fault is not an important structural element of the Krško basin. Moreover, from its geomorphic expression and its mapped length, it seems unlikely that it is a fault that is capable of generating earthquakes large enough to produce surface fault rupture. However, recent findings in the trench #2 at the Libna Hill indicate that the Libna fault may be described as capable if capability is defined in line with Safety guide SSG-9 (IAEA, 2010; where capability is not necessarily related to earthquakes on the fault of concern) and if the lower age-estimates of PI,Q formation are taken as relevant; because:

- The geologic buildup of the Libna hill is affected by strike-slip faulting, including deformation of the Globoko PlQ gravels and the overlying silts. Deformation is significant.
- The trench survey revealed a structural pattern in PlQ sediments (multiple fault traces close to the surface, complex branching pattern leading to an anastomosing geometry) that may be indicative of coseismic and recurrent displacements.
- One of more plausible interpretations is also that the observations are consistent with Post-Mousterien faulting on FZ1 (if inclusion of the Mousterien tool in the silty formation and within the FZ1 is interpreted as coeval) and also with Holocene coseismic deformation (if open cracks in FZ2 infilled by the organic soil are interpreted as coseismic).

The map locates the inferred capable fault inside the Sava plain into app. 200 m wide band, with its axis at only 250 meters and 500 meters (approximately) east of the eastern and western site fences, respectively. The capable fault then is not exactly crossing the eastern site project. Following the NRC regulation, we recommend investigating thoroughly especially nature and amount of displacement (kinematics, slip per event and cumulated slip), slip rate, estimation of recurrence interval and elapsed time since last event. Considering the strike-slip kinematics of the fault, we are aware that some of these tasks will be difficult to investigate and the results may not be conclusive, especially the data dealing with fault displacement and the age of the sediments.

We suggest that the location and geometry of faults along with the details of the spatial pattern of the fault zone (which may be important as they may define the particular locations where fault displacement may be expected) should be re-addressed. This latter topic is here particularly significant because of the short distance between the fault and the sites.

4.2 LIBNA FAULT AS A SECONDARY STRUCTURE, ACTIVATED BY A NEARBY SEISMIC SOURCE?

The external expert Daniela Pantosti suggests that the observed infiltrations of soil into the underlying sediment are infill of open cracks (see the trench 2 part of the report and Appendix 1), and that they could be secondary coseismic features due to a seismic event generated by another nearby fault. Additional actions are required to explore this possibility, the known fault sources that could be such "primary structures" are the Orlica and Artiče faults. The structural relation between the Libna fault and this nearby source fault (referring to the point (c) of the IAEA regulation guide) should then be explored.

4.3 LIBNA FAULT AS A SOURCE IN SEISMIC MOTION CALCULATION?

The Libna fault has so far been excluded from the seismogenic sources in PSHA, because there was no clustering of seismicity around it and its geometry could not have been associated with M>6 events, which are already included in the background seismicity. This position was based on the known length of the Libna fault (5 km) with its northern termination against the Orlica fault, and the southern termination underneath the Quaternary infill of the Krško basin against the inferred series of the so called "Balaton" faults, the latter being based on the geophysical data and the overall tectonic model.

From the new observations in the trench, we can argue that the width of the deformed zone is about 30 meters and it may also be larger, according to its "geophysical signature" (200 m.). According to scale relations (Scholz, 1997; Childs et al., 2009), such a large deformed zone may be associated with a cumulated slip ranging between 30 and 300 m. By applying another scale relation between cumulated slip and length of fault (Kim & Sanderson, 2005), the theoretical range of such a fault length should then be between 3 and 30 km. The conclusion from these relations is that the Libna fault length of 5 km is completely consistent with the available data, but a scenario with a longer fault is also possible (see the paragraph below).

Considering that the Libna fault is an active fault (affecting Plioquaternary and potentially also more recent layers), we conclude that the scenario with a 10 km long fault (continuation into the Gorjanci mts. into Malence fault and ending against the Čatež - Brvi structural zone; see Geology report of this project; Bavec, ed., 2010) cannot be conclusively discarded Thus, a consideration has to be made if it should be included in seismotectonic models in the lack of any discarding data, to comply with the philosophy of a conservative approach. The importance (weight) of such an option should then of course account for discarding the current tectonic model. However, we do not see the potential solution in simply adding the Libna fault into the current seismotectonic model as an option with significant probability. If attempts will be made in that direction, it should also be considered that the whole set of faults belonging to the same group as Libna (Sromljica, Močnik 1&2, Gabrnica, Trsnjak, Dramlja...) acts as a set of seismic sources of scattered seismicity, or a new tectonic and seismotectonic model will have to be built.

A possible solution to better constrain the geometry of the Libna fault south of its current termination is by a series of high resolution seismic lines across the continuation of its known trace.

In case of re-addressing the current tectonic model by additional investigations on the Libna fault, also a possibility of investigating its potential continuation across the Orlica fault should be considered. Current tectonic model (based on the regional geological knowledge and in this

particular part on the 1:5.000 non-reviewed manuscript geologic map) does not support such a solution, however the small alluvial plane disables the direct observations at the contact of the two faults.

4.4 ADDRESSING THE AMBIGUITIES

As previously mentioned with we recommend investigating the site vicinity for the capable fault issue even if conclusive results cannot be guaranteed beforehand.

1. In order to further assess the fault slip rate, we propose to continue the electrical mapping around trench 2 on the Libna hill. This approach gave encouraging results in 2009 and it will avoid to further excavation in the archeologically protected area.
2. We propose new trench(es) at the Libna foothills (not archeologically protected). With new trench(es) across Libna fault, we may hope to:
    a. Evaluate the activity of the fault in young colluvial deposits. By trenching, in the lower terrace that lies above the Sava plain, we may get the opportunity of cutting such young colluvium and to validate (or not) the different interpretations arising from the trench 2. The 2009 geophysical campaign (Mušič, 2009) revealed a potentially interesting site for trenching across the fault, with a clear NW-SE electric anomaly in the continuation of the trench 2 fault segment at the lowermost terraces in the southern foothills of the Libna hill.
    b. Examine the coseismic or aseismic character of the fault. It has not been completely possible in the excavated trench and there is no guarantee that new trenches will help but, as mentioned by Mc Calpin (2009), *"the degree to which coseismic fault slip can be distinguished from interseismic slip (creep) depends not only on the proportion of coseismic (morphogenic) to nonseismic slip but (as with the preservation of all paleoseismic evidence) on the relative rates of local processes."* So, two trenches in a very close perimeter can give drastically different information (e.g. Baize et al., 2010).
3. Concerning the potential continuation of the fault, we suggest to perform new high resolution seismic survey south of the Sava river (southern continuation of the Libna fault) and to carry out a morphotectonic analysis north of the Orlica fault (northern continuation).
4. There is no known absolute dating method that would guarantee (reliable) precise age dating of the deformed sediments in trench 2 on Libna and consequently the age of deformation. The age of deformation may be better constrained though if addressed by an extensive dating campaign in the Krško basin; dating all terrestrial formations; from Pl,Q to most recent ones by application of all available dating methods (U-series, cosmogenic nuclides exposure dating, OSL and ESR burial dating, radiocarbon...).

    As said, the tasks listed above are extensive and the results may not be conclusive. For that, a consideration can be made by the client to first evaluate a potential impact of the fault to the site by application of Probabilistic fault displacement hazard analysis (PFDHA) and only then to take a final decision on further field investigations.

5 CONCLUSIONS

The investigations performed by the consortium on the Libna fault, located near the two potential NPP II sites, show :

- The geologic buildup of the Libna hill is affected by strike-slip faulting, including deformation of the Globoko PI,Q gravels and the overlying silts. Deformation is significant.
- In lack of more constraining age - dates and other geologic information, the Libna fault should be considered capable if capability is defined in line with Safety guide SSG-9 (IAEA, 2010; that defines the recent activity of the fault by investigating its past activity as far back as to Pliocene and does not condition capability with seismic potential of the fault.)
- The structural pattern observed in the PIQ sediments may also be indicative of coseismic and recurrent displacements.

Results were not conclusive regarding *two topics:*

- The data does not allow distinguishing between the two alternative interpretations of the observed features in the trenches: the aseismic and the coseismic one.
- Comparison of various age dates of the Plio-Quaternary sediments in the area gives inconsistent results, which sheds doubts about the age of displacement along the Libna fault.

Additional investigations and analysis proposed in this report may lead to a better assessment of the potential impact of displacement along the Libna fault.

Concerning the assessment of the potential impact of the Libna fault to the two potential sites of concern the consortium has not found agreement on the consequences of the findings.

6 REFERENCES

Baize et al. 2010: Paleoearthquake evidences along the Pallatanga Fault (Ecuador), a segment of the Dolorès- Guayaquil-Megashear. ESC 32nd General Assembly, Montpellier (France), 6-7 september.

Bavec, M. 2000: Poročilo o določanju starosti kvartarnih sedimentov v Krški kotlini z metodo termoluminescence (TL) in optično stimulirane luminescence (OSL). Projektna naloga: Neotektonske raziskave na območju JE Krško. Naročnik Uprava RS za jedrsko varnost. - Tipkano poročilo. Geološki zavod Slovenije.

Bavec, M. (ed.) 2008: Paleoseismological investigations of the Libna fault. Trench in Stari Grad. – Project report for Geotechnical, Geological, and Seismological (GG&S) Evaluations for the New Nuclear Power Plant at the Krško Site (NPP Krško II); tasks 4.3.1.c, 4.3.1.c1, 4.3.1.d; 22pp, 5 appendices.

Bavec, M., Rižnar, I., Jež, J., Novak, M. 2008: Geološka spremljava v okviru varstva naravne dediščine - strukturno tektonske značilnosti na območju trase in spremljajočih objektov na AC Vrba - Črnivec (Peračica).) - Tipkano poročilo, 64 str. Geološki zavod Slovenije.

Bavec, M. (ed.) 2010: Geotechnical, geological and seismological (GG&S) evaluations for the new nuclear power plant at the Krško site (NPP Krško II), Geology : phase 1 : revision 1. Ljubljana: Geological Survey of Slovenia, 2010. 178 pp.

Childs et al. 2009: A geometric model of fault zone and fault rock thickness variations. Journal of Structural Geology, 31, 117–127.

Grad, K., Ferjančič, L., 1974: Osnovna geološka karta SFRJ, list Kranj, 1:100.000. Zvezni geološki zavod, Beograd

IAEA 2003: Site Evaluation for Nuclear Installations", IAEA SAFETY STANDARDS SERIES, SAFETY REQUIREMENTS No. NS-R-3, Vienna, INTERNATIONAL ATOMIC ENERGY AGENCY.

IAEA 2010: Seismic Hazards in Site Evaluation for Nuclear Installations", IAEA SAFETY STANDARDS SERIES, Specific Safety Guide No. SSG-9, Vienna, INTERNATIONAL ATOMIC ENERGY AGENCY.

Kim and Sanderson. 2005: The relationship between displacement and length of faults: a review. Earth-Science Reviews, 68, 317–334.

Lai, Z. P. 2010: Chronology and the upper dating limit for loess samples from Luochuan section in the Chinese Loess Plateau using quartz OSL SAR protocol. - Journal of Asian Earth Sciences 37 (2010) 176–185.

Lee, J. C., Rubin, C., Mueller, K., Chen, Y. G., Chan, Y. C., Sieh, K., Chu, H. T., and Chen, W. S. 2004. Quantitative analysis of movement along an earthquake thrust scarp: A case study of a vertical exposure of the 1999 surface rupture of the Chelungpu fault at Wufeng, western Taiwan. J. Asian Earth Sci. 23, 263–273.

Lienkaemper, J. J., Dawson, T. E., Personius, S. F., Seitz, G. G., Reidy, L. M., and Schwartz, D. P. 2002. A record of large earthquakes on the southern Hayward fault for the past 500 years. Bull. Seis. Soc. Am. 92(7), 2637–2658.

Lienkaemper and Williams 2007. A record of large earthquakes on the southern Hayward fault for the past 1800 years. Bull. Seis. Soc. Am., 97, 1803-1819.

Lienkaemper, J.J., Sickler, R.R., Brown, J. and Baldwin, J.N. 2011: A Record of Large Earthquakes on the Green Valley Fault for the Past Millennium. - Bull. Seis. Soc. Am., Submitted; ftp://ehzftp.wr.usgs.gov/jlienk/gvf/BSSA-D-11-00nnn-esupp/BSSA-D-11-00nnn-esupp.html.

Lowick, S. E., Preusser, F. and Winkle, A. G. 2010: Investigating quartz optically stimulated luminescence doseeresponse curves at high doses. - Radiation Measurements 45, 975-984.

Lowick, S. E., Preusser, F., Pini, R. and Ravazzi, C. 2010b: Underestimation of fine grain quartz OSL dating towards the Eemian: Comparison with palynostratigraphy from Azzano Decimo, northeastern Italy. - Quaternary Geochronology 5, 583–590

Lowick, S. E. and Preusser, F. 2011: Investigating age underestimation in the high dose region of optically stimulated luminescence using fine grain quartz. - Quaternary Geochronology 6, 33-41.

McCalpin, J. P. (2005a). Late Quaternary activity of the Pajarito fault, Rio Grande rift of northern New Mexico, USA. Tectonophys. 408, 213–236.

McCalpin. 2009: Paleoseismology. Academic Press, 629 pages.

Meghraoui and Doumaz 1996. Earthquake-induced flooding and paleoseismicity of the El Asnam (Algeria) fault-related fold. J. Geophys. Res., 101, 17,617 – 17,644.

Miall. 1977: A review of the braided river depositional environment: Earth Science Review, 13, 1-62.

Mušič 2009: Report on ground penetrating radar and resistivity survey. Libna, Oct. 2009. - Internal report, Gearh d.o.o

Philip, H., Rogozhin, E., Cisternas, A., Bousquet, J. C., Borisov, B., and Karakhanian, A. (1992). The Armenian earthquake of 1988 December 7: Faulting and folding, neotectonics and paleoseismicity. Geophys. J. Int. 110, 141–158.

Piller, W.E., Mathias Harzhauser, M. and Mandić, O. 2007: Miocene Central Paratethys stratigraphy – current status and future directions. Stratigraphy, 7, 151 – 168.

Premru, U., 1983: Osnovna geološka karta SFRJ, list Ljubljana, 1:100.000. Zvezni geološki zavod, Beograd

Rakić, M., P. Stejić, P. and Simonović, S. 2002: Palaeogeography of Southeasteren Part of Pannonian Basin During Pliocene and Quaternary. – Geologica Charpatica 53, Special Issue. Proceedings of XVII. Congress of Carpathian-Balkan Geological Association Bratislava.

Rižnar, I., Koler, B. & Bavec, M. 2005: Identifikacija potencialno aktivnih struktur vzdolž reke Save na podlagi topografskih podatkov in podatkov nivelmanskega vlaka. (Identification of potentially active structures along the Sava River using topographic, and leveling line data). – Geologija 48/1, 107-116, Ljubljana.

Scholz. 1997: Scaling properties of faults and their populations. Int. J. Rock Mech. & Min. Sci, 34, 3-4.

Swan, H. B., Hanson, K.L., Poljak, M., Živčič, M. & Gosar, A. 2004: Revised Seismotectonic Model of the Krško Basin, Part 1, PRS-NEK 2.7.1 rev. 1. prepared for Nuclear Power Plant Krško, Vrbina 12, Krško, Slovenia; by Geomatrix Consultants, Inc, Oakland, California, USA; in cooperation with University of Ljubljana, Faculty of Civil and Geodetic Engineering Institute of Structural Engineering, Environmental Agency of the Republic of Slovenia, Office of Seismology; and Geological Survey of Slovenia.

Šikić, K., Basch, O., Šimunić, A., 1979: Tumač za list Zagreb L 33-78. Osnovna geološka karta SFRJ 1:100.000. Savezni geološki zavod, Beograd.

Verbič, T., 1995, Kvartarni sedimenti v vzhodnem delu Krške kotline: Unpublished report, št. dok. ŠGGS7, 248 p.

Verbič, T. 2004: Stratigrafija kvartarja in neotektonika vzhodnega dela Krške kotline. 1. del: stratigrafija. (Quaternary stratigraphy and neotectonics of the Eastern Krško Basin. Part 1: Stratigraphy). – Razprave IV Razreda SAZU XLV-3, 171-225, Ljubljana (Abstract in English).

Verbič, T., 2005: Stratigrafija kvartarja in neotektonika vzhodnega dela Krške kotline. 2. del: neotektonika. (Quaternary stratigraphy and neotectonics of the eastern Krško basin. Part 2: Neotectonics.) - Razprave IV. Razreda Sazu, vol. XLVI-1, 171-216, LJubljana (Abstract in English).

Wells and Coppersmith 1994: New empirical relationships among magnitude, rupture length, rupture width, rupture area and surface displacement. Bull. Seism. Soc. America, 84, 974-1002.